Microsystem Technologies (2022) 28:1077–1114
https://doi.org/10.1007/s00542-022-05265-0

REVIEW PAPER

Current innovations in roller embossing—a comprehensive review

Swarup S. Deshmukh[1] · Arjyajyoti Goswami[1]

Received: 5 July 2021 / Accepted: 17 February 2022 / Published online: 10 March 2022

Abstract

Hot embossing (HE) is a micro-manufacturing technique used to develop micro and nano-scaled patterns over a polymer workpiece. The traditional-HE process is only partially implemented in micro-manufacturing industries owing to limitations like low productivity due to batch-wise manufacturing and high processing time. But presently, the demand for large-area patterned polymer substrate is rising due to its applications in diverse areas like displays, micro-lenses, anti-reflection films, micro-fluidic devices, self-cleaning surfaces, etc. Therefore, the traditional hot embossing (HE) process has been modified to the roller hot embossing (RHE) process to meet the increased demand. The RHE process is categorized into the roll-to-plate (R2P) and roll-to-roll (R2R) process. The present paper comprehensively reviews the different advancements in setups of the roll-to-plate (R2P) and roll-to-roll (R2R) hot embossing for large-scale fabrication of micro and nano-sized patterns over the polymer substrate. The graphical, numerical and statistical analysis shows that majorly ultraviolet (UV) lithography/X-ray lithography/electron beam lithography followed by Ni-electroplating/reactive ion etching/wet etching are the most commonly utilized techniques for mold manufacturing. But due to its complexity, researchers have slowly moved towards non-conventional machining processes for mold fabrication i.e., micro-EDM, micro-milling etc. According to a graph showing the percentage distribution of work associated with recent advancements in roller hot embossing, the thermal assisted R2R-HE is the most popular, followed by UV aided R2R-HE, and inductive aided R2R-HE, respectively. The thermal assisted R2R-HE contributes 36% of total innovations in RHE followed by UV aided R2R-HE (14%), and inductive aided R2R-HE (10%).

Abbreviations

R2R-HE	Roll to roll hot embossing
R2P-HE	Roll to plate hot embossing
HE	Hot embossing
UV	Ultraviolet
IR	Infrared
T_g	Glass transition temperature
T_o	Room temperature
T_e	Embossing temperature
T_m	Melting temperature
P_e	Embossing pressure
μ	Micro
R_a	Surface roughness
PMMA	Polymethyl methacrylate
PC	Polycarbonate
PET	Polyethylene terephthalate
COC	Cyclic-olefin-copolymer
FEA	Finite element analysis
EDM	Electric discharge machining
FIB	Focused ion beam
AAO	Anodic aluminium oxide
ECDM	Electro chemical discharge machining
EBW	Electron beam writing
PCB	Printed circuit board
UV/X-ray/ EBL	UV lithography/X-ray lithography/ Electron beam lithography
NE/RIE/WE	Ni electroplating/ Reactive ion etching/Wet etching

✉ Arjyajyoti Goswami
arjyajyoti.goswami@me.nitdgp.ac.in;
aj87.goswami@gmail.com

Swarup S. Deshmukh
deshmukh.swarup@gmail.com;
dss.19me1106@phd.nitdgp.ac.in

[1] Department of Mechanical Engineering, National Institute of Technology, Durgapur, West Bengal 713209, India

1 Introduction

The requirement for patterned polymer has been rising continually in present times because it fulfills the need for commercial applications in various domains like optics,

biomedical, and MEMS (micro-electro-mechanical systems). The most common approaches to fabricate micro patterns on polymer substrates are micro-injection molding (Piotter et al. 2002; Su et al. 2003; Shen et al. 2007; Huang and Tai 2009; Kim et al. 2013a) and hot embossing (Heckele et al. 1998; Juang et al. 2002a, b; Li et al. 2005; Pan and Su 2008a, b; Wong et al. 2010; Weng et al. 2011; Park et al. 2011). Compared to micro-injection molding, reduced residual stresses in the end product were observed through hot embossing. In addition, the temperature deviation in hot embossing (HE) is lower in contrast to micro-injection molding (Heckele et al. 1997; Schift et al. 2000; Mekaru et al. 2004; Wu and Kuo 2007).

Hot embossing (HE) is a micro-manufacturing method mainly used to fabricate micro(μ)/nano-scaled patterns over a heated thermoplastic polymer by applying optimum pressure on the mold (Jaszewski et al. 1998; Becker and Dietz 1998; Scheer and Schulz 2001). Hot embossing is categorized into two groups: traditional hot embossing and roller embossing. The polymer web/substrate is positioned over the hot plate/bottom plate heated via a pencil heater in traditional hot embossing. This polymer web/substrate is positioned beneath the micro-patterned mold, and during the embossing stage, the optimum value of pressure was applied over the mold. Consequently, the micro-patterns over the mold are replicated over the polymer web/substrate (Becker and Heim 2000; Worgull et al. 2005, 2006; Kolew et al. 2011; Deshmukh and Goswami 2020b). The traditional hot embossing (HE) system is illustrated in Fig. 1a. There are various micro-manufacturing processes like UV/X-ray/electron beam lithography (EBL) followed by nickel electroplating or reactive ion etching (RIE) (Chien 2006; Mappes et al. 2008; Wu et al. 2010b; Schelb et al. 2011; Yang et al. 2014), micro-milling (Gerlach et al. 2002; Hupert et al. 2006; Forfang et al. 2014; Zhang et al. 2014a), micro-electric discharge machining (μ-EDM) (Kimerling et al. 2006), focused ion beam (FIB) machining (Bhavsar et al. 2012; Goswami et al. 2017, 2018), laser engraving (Niino et al. 2004; Cheng et al. 2014; Zhu et al. 2017; Deshmukh and Goswami 2020a), electric discharge machining (EDM) (Ali and Mohammad 2009; Li et al. 2018), CNC-Milling (Gomez et al. 2014), wire electric discharge machining (WEDM) (Li et al. 2020), electrochemical discharge machining (ECDM) (Kumar et al. 2020), etc. that the researchers have used for fabricating micron-sized patterns over the surface of the mold. In addition to this, the micro-sized patterns can also be developed through 3-D printing (Lin et al. 2017), anodic aluminum oxide process (Wu et al. 2010a; Chuang et al. 2018), and polydimethylsiloxane (PDMS) casting (Kim et al. 2013b). Recently a variety of different molds have been used for embossing. Notable amongst them are micron-scaled hot wire, i.e., metal wire with micron-scale diameter heated above Tg of the polymer workpiece (Gan et al. 2010), printed circuit board (PCB) (Chee et al. 2013), elastomeric mold(Zhong et al. 2018) and shark-skin(Park and Kim 2014) having randomly arranged rib patterns which helps them in faster and more efficient swimming; have been directly used as a mold in traditional hot embossing.

The literature review concludes that the traditional hot embossing (HE) is a low throughput process due to limited patterning area, batch-wise operation, and long processing time. In addition, in traditional hot embossing, the pressure exerted throughout the embossing is shared non-uniformly, which influences the precision of the embossed micro-patterns (Deshmukh and Goswami 2021). To overcome these issues, researchers have designed and developed various setups like gas-pressurized hot embossing (Chang and Yang 2003; Chang et al. 2006a; Hocheng et al. 2008; Wan et al. 2016), micro (μ)-powder hot embossing (HE) (μ-Powder HE) (Sahli et al. 2010; Sahli and Gelin 2013; Zhang et al. 2013, 2015; Emadinia et al. 2020), inductive hot embossing (Nian et al. 2016; Shih et al. 2017; Kao et al. 2020; Deshmukh and Goswami 2022), hot fluid-based hot embossing (Chang and Yang 2005), laser-assisted hot embossing (Kurita et al. 2018), infrared-based hot embossing (Chen et al. 2014), ultrasonic hot embossing (UHE) (Mekaru et al. 2007, 2008; Jung et al. 2012, 2015; Seo and Park 2012; Tsai et al. 2012; Qi et al. 2015, 2013; Lee and Park 2014, 2016; Liao et al. 2015; Kosloh et al. 2017a, b; Zou et al. 2019; Sucularli et al. 2020), carbon-dioxide based hot embossing (Yang et al. 2008; Huang et al. 2009; Weng and Huang 2013), and low force hot embossing (He et al. 2015), etc. Roller embossing is categorized into two types based on the heating of the polymer substrate. The first one is thermally assisted roller embossing, and the second one is UV roller embossing. The setup of thermally assisted roller embossing and UV roller embossing is depicted in Fig. 1b and c, respectively.

In thermally-assisted roller embossing, the roller mold is usually heated with a heating coil, inductive/infrared heater, etc. The roller mold is generally designed by wrapping the belt mold or flat mold having micro-patterns over it on the roller or fabricating the micro (μ)-patterns over the roller surface directly. Then, the micro-patterns on the roller mold are replicated/copied over the thermoplastic polymer substrate/web by heating the roller mold higher than the T_g of the polymer substrate/web and applying an optimum value of pressure over the roller mold. This is because the thermoplastic polymer has a higher viscosity at T_o. Therefore, heat is usually added to increase the substrate's temperature beyond the T_g to flow the polymer material in the micropattern's cavity over the mold under the applied pressure. Polycarbonate (PC), PMMA (Polymethyl methacrylate), PE (Polyethylene), PS (Polystyrene),

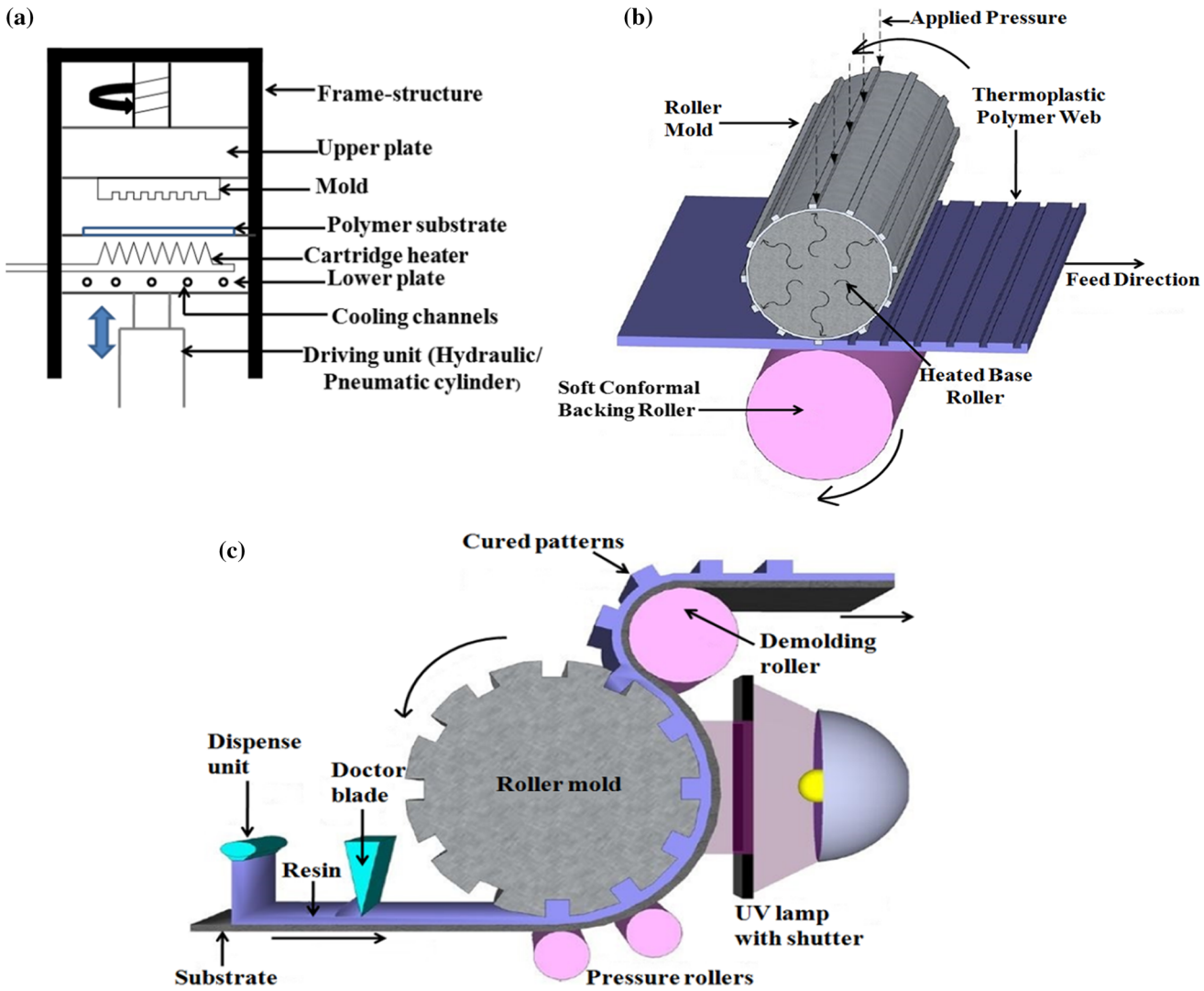

Fig. 1 **a** Traditional hot embossing, **b** Thermally assisted roller embossing, and **c** Ultraviolet (UV) roller embossing (Dumond and Yee Low 2012)

PET (poly-ethylene-terephthalate), COC (cyclic-olefin-copolymer) are some of the commonly used thermoplastic polymer workpieces/web in the thermally-assisted roller embossing.

In ultraviolet (UV) roller embossing, the UV-curable resin having low viscosity is deposited over the polymer web/substrate and cured through an UV light source (Zhong et al. 2011; Song et al. 2015). Adding UV curable resin coat over the substrate adds some external complications to the process. This external complication includes the need for standardized deposition and spreading mechanism and maintaining the proper adhesion of the coat to the substrate. These difficulties have been compensated by performing the UV roller embossing at room temperature and low embossing pressure. A dispensing device was employed to spread the UV curable resin over the polymer web (Ahn et al. 2006, 2007a). The thickness of the coating was controlled through a doctor's blade. The coating thickness can be indirectly regulated by altering the dispensing rate, the viscosity of the UV curable resin, the diameter of the dispensing head diameter, and the polymer's web/ substrate feed rate. Alternately the coating of UV curable resin may be applied over the polymer web by using the coating roller. This coating roller is prepared by dipping the roller into a basin of UV curable resin, but this technique is less flexible for thickness control (Ahn et al. 2007b; Ahn and Guo 2008, 2009). The dispensing unit is computer-controlled to coat an appropriate area of the polymer substrate as per requirement. In UV roller embossing, the roller mold is compressed against the substrate coated through UV curable resin, followed by the curing process. Monomers like acrylic or epoxies were generally coated over the surface of the web. These monomers absorb the UV light; that's why polymerization

reaction occurs. It alters the hardness as well as the flexibility of coating of the UV curable resin. In addition to this, reactive dilutants and special additives were added to UV curable resin. It helps alter properties like viscosity, wetting property for adhesion over specific polymer surface, and polymer hardness after curing.

Furthermore, a fluorinated group in UV curable resin enhances the anti-sticking property to avoid UV curable resin sticking to the mold. The UV roller embossing has been carried out at low pressure and ambient temperature; soft embossing materials like polydimethylsiloxane (PDMS) can be implemented for embossing, even though conventional nickel molds to be commonly employed. With its lightweight mold and substrate content, UV roller embossing is a particular technique that is nearly robust. With the commonly known caution, at least one mold or workpiece/web needs to be translucent to UV light such that the resin is fully cured.

There are a few similarities and differences between traditional hot embossing and roller embossing. The similarities are summarized as follows-

(1) Both methods use a patterned mold to emboss the micro-patterns over the substrate surface either by utilizing the heat energy or the UV energy together with the optimum value of pressure.
(2) In both methods, it is necessary to implement a smooth mold with a lower surface roughness value (R_a) and flat polymer substrate to emboss the micropattern without distortion in the features and avoid partiality filling. In roller embossing, ideally, it is necessary to implement the roller with no surface waviness, but it is pretty challenging to obtain in reality. In UV roller embossing, it is essential to coat the polymer web/workpiece uniformly with the UV resin; it is influenced by the flatness of the polymer web/workpiece.
(3) For the traditional hot embossing and roller embossing, identical embossing media, i.e., polymer workpiece, are used, but the roller embossing approaches primarily focus on the embossing speed. Polyethylene terephthalate (PET), PMMA (polymethyl methacrylate), as well as PC (polycarbonate) are mainly used as embossing media in both methods. But in UV-assisted roller embossing and UV-assisted traditional embossing, UV curable resin is used as working media. In UV-assisted traditional hot embossing, UV curable resin is coated over the polymer workpiece through spin coating. While in UV roller embossing, the UV curable resin is coated over the substrate through inkjet printing or spray coating or with the help of a coating roller. In both methods, for high precision and filing of microcavities during embossing, it is necessary that the working media, i.e., polymer substrate and UV curable resin, should have an excellent viscoelastic property.

There are also significant differences between continuous roller embossing and the traditional hot embossing, which are as discussed below:

(1) In roller embossing, the necessary pressure is applied exclusively along with the roller and the polymer media contact line. While in traditional hot embossing, pressure is applied over the mold. Thus, the entire micro-pattern on the mold is replicated simultaneously over the polymer substrate. In traditional hot embossing, minor surface contour variations between mold and polymer surface or dust motes may affect the embossing area. This may produce distortions in the embossed micropattern and high-stress levels in the mold that cause deformation or mold deterioration. In traditional hot embossing, multiple tonnes of forces are applied over the mold to replicate the whole micro-pattern over the thermoplastic film. In roller embossing, the force needed to transfer the micropattern is considerably decreased due to the surface upon which pressure is being exerted is much smaller. The decreased force reduces the risk of mold warping substantially, eases the design, and developed an effective roller embossing setup.
(2) In traditional hot embossing, nonstick coatings are commonly applied over the mold surface due to high surface energy to reduce the deembossing force during the deembossing stage. While in roller embossing, just the line width underneath the roller is embossed at any point, hence the forces needed to separate the mold are significantly reduced. However, the non-stick coating over the mold surface is restricted for the UV roller embossing because it may lead to polymerization reaction with UV curable resin. So in the case of UV roller embossing, it is preferable to fabricate the mold with low surface energy material like PDMS rather than metallic mold to prevent deterioration of embossed micro-pattern throughout the deembossing stage.
(3) In roller embossing, even if air gets trapped between the line contact of roller mold and polymer workpiece, the applied pressure helps in squeezing it out along an instant exit direction on all sides of the contact line. In traditional hot embossing, if air gets trapped underneath the mold area, there is no quick exit route for the trapped air. This trapped air generates an air bubble which ultimately distorts the embossed micropatterns over the polymer surface.

(4) Vertical deembossing for traditional hot embossing is usually favored to mitigate the distortion of structure and failure induced by shear stresses exerted by the mold lateral resistance movement. As such vertical deembossing is difficult in roller embossing, deembossing becomes a separation flake off the mold and polymer substrate at a particular angle; it relies on the roller mold diameter. So it is necessary to select the right diameter of the roller mold.

(5) Some compromises are needed in the speed of roller embossing to achieve precision in the embossed micro-pattern. It is not usually feasible to achieve nano-scaled accuracy in roller embossing with a flexible mold because deformation and distortion occur in the flexible mold during the deembossing stage.

1.1 Motivation and contribution

Traditional-HE/Plate-to-plate-HE is only partly adopted in micro-manufacturing companies because of few restrictions including poor productivity because of batch-wise production and long processing times. Traditional hot embossing is inadequate for applications needing a large embossed area at a reasonable cost because of the restricted embossing area. Because of this, hot embossed patterns used in displays and microlenses, anti-reflection film, backlight devices, and hydrophobic surfaces etc., cannot be produced with traditional hot embossing. So, Roller embossing was developed to address these concerns. This review article provides detailed path for upcoming researchers/scientists who want to work in the field of roller hot embossing. This article describes various types of roller hot embossing and how it differs from the traditional hot embossing. This review article also deals with the latest innovations in the roller embossing setups which have been made to overcome few limitations/problems that were observed in the initial stages of the roller embossing setup development by different researcher groups. This review gives brief idea about the commercial applications of roller embossing in the various domains where it is mainly used.

The present article is structured as follows: the different types of thermoplastic polymers utilized in the roller embossing process and their deformation behavior during the process is discussed in Sect. 2. Section 3 reviews the detailed classification of roller embossing as per the tool configuration and setup design. Section 4 discusses recent improvements or adjustments made by researchers to address several challenges (long cycle time and viscoelastic recovery) that were observed in the early stages of roller embossing setup development. Section 5 summarizes the commercial applications of roller embossing in the various domains. The critical analysis of various roller embossing setups i.e. their need, effectiveness and limitations is discussed in Sect. 6. The direction for the future research in the field of roller embossing is presented in the Sect. 7. Section 8 concludes summary of review article in graphical, numerical and statistical format. It is intended to help the researchers/scientist/readers to analyze data related to recent innovations in roller embossing in a concise but comprehensive way. Finally few concluding remarks are drawn in the Sect. 9.

2 Various polymers for the hot embossing process and its deformation behavior

Generally, the thermoplastic polymer is mainly used as a substrate during the hot embossing process. Thermoplastic polymers are the most preferred materials for hot embossing because of their inexpensive cost, lightweight, low molding temperature, and wide range of thermal, optical, and chemical characteristics. Amorphous polymers and semi-crystalline polymers are the two types of thermoplastic polymers. Based on their thermal stability, each group is further divided into three types: standard, technical, and high-performance polymer. The detailed classification of thermoplastic polymer is shown in Fig. 2. Amorphous polymer is most commonly used in optical applications like Fresnel lenses, an optical diffuser, microlenses, etc. An amorphous polymer has high transparency compared to a semi-crystalline polymer. The most commonly served amorphous polymer as a substrate during hot embossing are PC (polycarbonate), PMMA (Polymethyl methacrylate). Due to crystalline part in semi-crystalline polymer causes significant refraction it affects the transparency. At the same time, the semi-crystalline polymer has a highly chemical-resistant property. As a result, it is mainly used to fabricate the microfluidic chip used for cell culturing, DNA (deoxyribonucleic acid), and RNA (ribonucleic acid) test, manufacture micro-container for oral drug, micro-needles, etc. The most commonly used semi-crystalline polymers in hot embossing are PP (Polypropylene), PET (Polyethylene terephthalate), and PEEK (Polyether ether ketone). The thermoplastic polymer has viscoelastic characteristics, i.e., it shows the elastic as well as viscous property.

During hot embossing, the thermoplastic polymer is deformed in the three states glassy, rubbery, and flow concerning temperature it is depicted in Fig. 3. The polymer workpiece is deformed in the glassy region when the working temperature is less than the T_g. This deformation is fully elastic and is caused by the lengthening of the atomic distance. As the operating temperature rises and

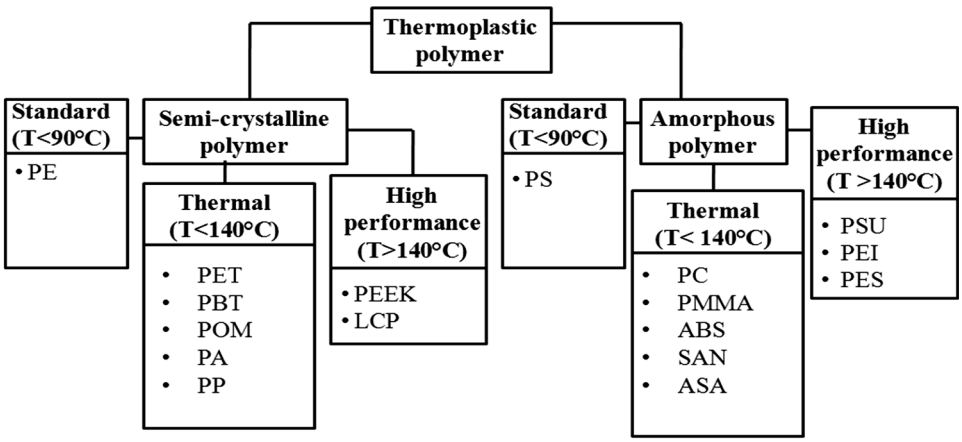

Fig. 2 Detailed classification of thermoplastic polymer

PE: Polyethylene, **PET:** Polyethylene terephthalate, **PBT:** Polybutylene terephthalate, **POM:** Polyoxymethylene, **PA:** Polyamide, **PP:** Polypropylene, **PEEK:** Polyether ether ketone, **LCP:** Liquid-crystal polymer, **PS:** Polystyrene, **PC:** Polycarbonate, **PMMA:** Polymethyl methacrylate, **ABS:** Acrylonitrile butadiene styrene, **SAN:** Styrene acrylonitrile resin, **ASA:** Acrylonitrile styrene acrylate, **PSU:** Polysulfone, **PEI:** Polyethylenimine, **PES:** Polyethersulfone.

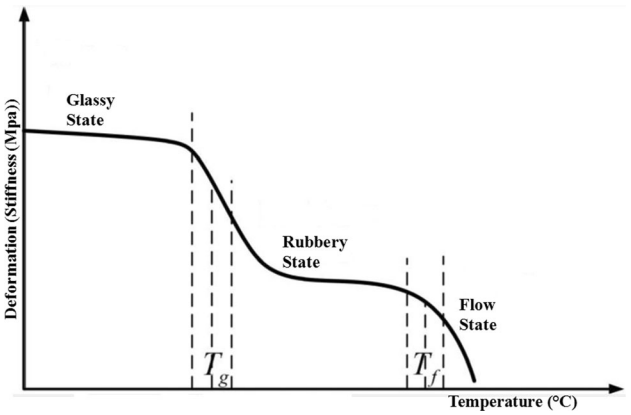

Fig. 3 Deformation behavior of thermoplastic polymer with respect to temperature during hot embossing (Peng et al. 2016)

goes beyond the T_g the polymer substrate reaches the rubbery region. The substrate takes on a rubber-like quality in this region, becoming soft and acting like incompressible rubber. The deformation of the polymer in the rubbery region is caused by the localized displacement of the polymer chain. Therefore, its stiffness is significantly lowered, making the deformation of the polymer workpiece much easier. Close to the T_g vibration motion of polymer molecule rises, and heat energy is enough to cover the obstacle to transverse and longitudinal movement of the polymer molecule. Therefore polymer molecules easily travel from one lattice to the next lattice, resulting in a material becomes rubbery. As a result, the deformation of the substrate is easier in the rubbery region than glassy region. Despite this, the transient network of entanglements continues to hold whole chains together. In the rubbery condition, the deformation will restore once the load is released. With the temperature rise, the polymer substrate attains the flow region. In this region, polymer chains get displaced due to chain sliding. Therefore stiffness and viscosity of polymer substrate reduced drastically, and its deformation is entirely irreversible.

The polymer substrate is heated above T_g and below T_m throughout the embossing process to avoid flaws. As a result, embossing is done in a rubbery region. Therefore, this recoverable deformation in the rubbery region has a considerable impact on the embossed part's accuracy. There are two ways to prevent recoverable deformation in the rubbery region. The first approach involves rapidly cooling the polymer substrate throughout the deembossing stage, whereas the second approach involves disentangling polymer chain fragments to achieve permanent deformation.

3 Classification of roller embossing

The roller embossing is classified into two types based on the embossing tool's configuration and setup design. The first one is the roll-to-plate hot embossing (R2P-HE), and the other is the roll-to-roll hot embossing (R2R-HE). The detailed classification of roller embossing is shown in Fig. 4.

(1) Roll-to-plate hot embossing (R2P-HE)

Plate-to-plate hot embossing (P2P-HE)/ traditional hot embossing cannot fabricate micro-patterns with a complex profile on a large area of the polymer workpiece. Moreover, being a batch-wise manufacturing approach, traditional hot embossing faces issues like low throughput,

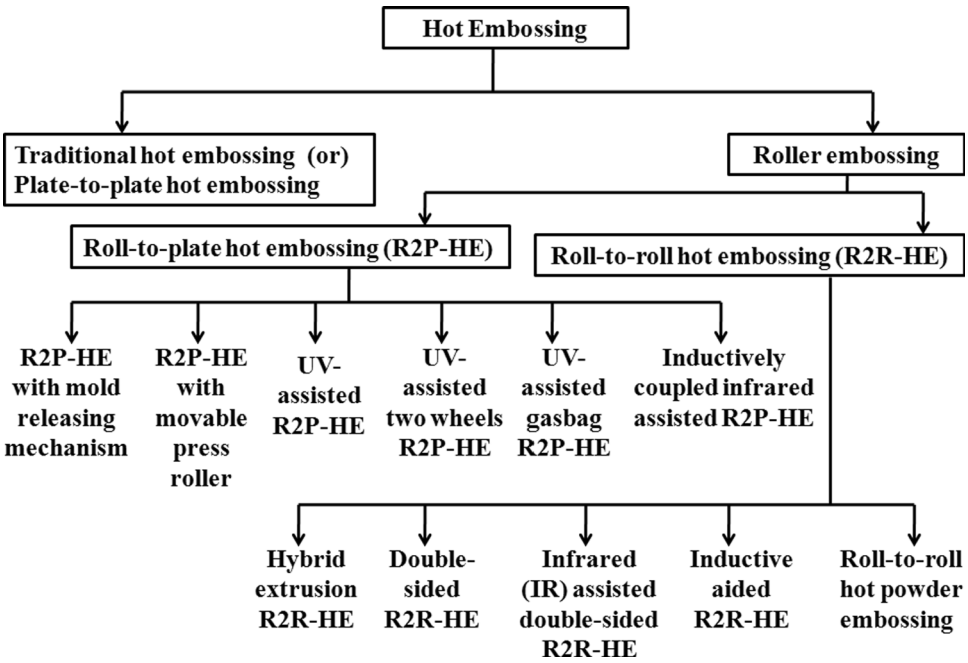

Fig. 4 Detailed classification of roller embossing

small embossing area, lower manufacturing efficiency, etc. To solve these issues, roll pressing hot embossing processes, i.e., R2P-HE and R2R-HE processes, were developed. This process has numerous advantages like better replicability, high throughput, high manufacturing efficiency, simple setup, and cheap cost.

In 1998 Tan et al. (1998) initially suggested the idea of roll-to-plate hot embossing. As per his idea, two setups related to roll-to-plate hot embossing were developed. The first setup of a roll-to-plate hot embossing (R2P-HE) with roller mold is depicted in Fig. 5a. The mold was wrapped around the roller called roller mold, and the substrate was placed on a heated moving plate on which the embossing was carried out. The second setup of a roll-to-plate (roller to plate) hot embossing with flat mold is depicted in Fig. 5b. The flat mold (usual mold consists of a micro-pattern) is placed on a polymer substrate (polymer workpiece) positioned on a moving hot plate, and a plain heated roller moves on the mold. As a result that, micro-patterns present on flat mold are embossed over polymer workpiece under roller pressure. In both setups, the roller temperature was fixed higher than the T_g of the polymer web/ workpiece, and the temperature of the moving hot plate was set at a value less than the T_g.

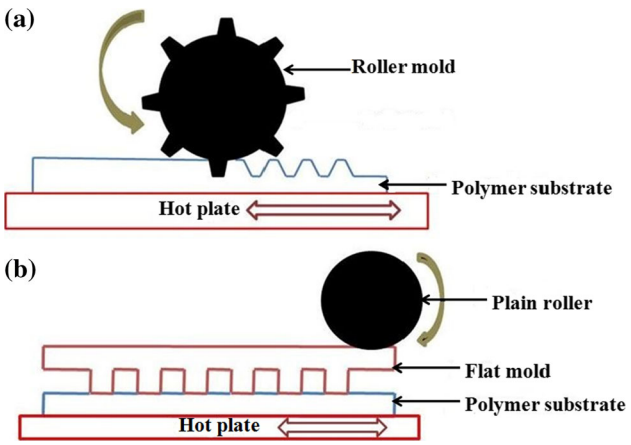

Fig. 5 **a** Roll to plate hot embossing with roller mold, and **b** Roll to plate hot embossing with flat mold

The polymer workpiece in touch with the roller has a temperature greater than T_g that softens that area. Finally, due to applied pressure, the micro-patterns over the mold are embossed only over the selected region on the polymer material. This process is different from the P2P-HE in which the whole polymer web/substrate is embossed at a time, and applied load is kept constant until the temperature of the polymer workpiece attains the de-embossing temperature. Using this roll to plate hot embossing setup, nano-metric scale patterns were successfully embossed on a polymer workpiece. Guo et al. (2004) fabricated nano-scaled pillar patterns on a polycarbonate substrate using a roll-to-plate hot embossing with roller mold setup. Well replicated nano-scaled patterns were observed at an embossing temperature of 150–170 °C, and applied pressure was in the range of 2.1×10^5 to 3.3×10^5 Pa. Nano-metric sized pores arranged in a hexagonal arrangement were developed on an aluminum roller through anodic oxidation of aluminum. Wettability assessment was done by calculating the contact angle (CA) of water over the surface. It has been found that when the diameter of the nano-pillar reduces, the contact angle rises. The outcomes

of the SEM (scanning electron microscope) as well as XPS (X-ray photoelectron spectroscopy) confirmed that the fraction of air in troughs between individual nano-pillar and reorientation of molecules on the embossed surface was responsible for the enhancement in contact angle (CA), i.e., a transformation of a surface from hydrophilic to a hydrophobic.

Shuhuai Lan et al. (2010) pointed out that related to R2P-HE, less work has been done regarding the filling mechanism of micro/nano-sized cavities on the mold. For that reason, a numerical model was developed according to the Navier–Stokes equation and Hertz contact pressure distribution. This model was used to predict the polymer flow in micro-nano-sized cavities on the mold throughout the R2P-HE. The geometrical configuration considered for the analytical model of R2P-HE with flat mold process and polymer flow in micro/nano size cavities on the flat mold during embossing is illustrated in Fig. 6a and b, respectively. This numerical model gives the interconnection between the operating parameters and replication ratio (ratio of the height of polymer flow in micro/nano size cavity on the mold during the roll-to-plate (roller to plate) hot embossing (ΔZ) to the height of micro/nano size cavity on the mold (H)) obtained after the hot embossing. The final result of this numerical model is given in Eq. 1 (Lan et al. 2010).

$$R_{replication} = \frac{1}{R_{aspect}} \left(\frac{-\overline{P}a}{12\vartheta\eta} \right)^{1/2} \quad (1)$$

where, $R_{replication}$ = replication ratio = $\frac{\Delta Z}{H}$; R_{aspect}=$\frac{H}{W}$, (W = width of micro-pattern); $\overline{P}$ = average pressure on roller = $\frac{F}{La}$; F = applied force on the roller, L = width of the roller and flat mold, a = contact length of the roller; η= viscosity of polymer substrate; ϑ = moving speed of flat mold.

For the validations of this numerical model, a set of experiments were conducted on an in-house developed experimental setup shown in Fig. 6c. It had a steel roller equipped with a heating element in the core, flat mold. It was also equipped with a heater to heat the polymer substrate above T_g, linear gripper, and tension roller incorporated to retain the space within the mold and the polymer. The replication ratio of embossed patterns was calculated and compared with the results predicted by the numerical model. It was seen that there is a close deal between the experimental result and the numerically forecasted result. It is noticed that better replicability was obtained at the lowest roller speed and highest average pressure. This is because the molten polymer gets more time to fill the mold's micro/nano-sized cavities at lower roller speeds. While at a higher value of moderate pressure, the applied force efficiently presses the molten polymer inside the

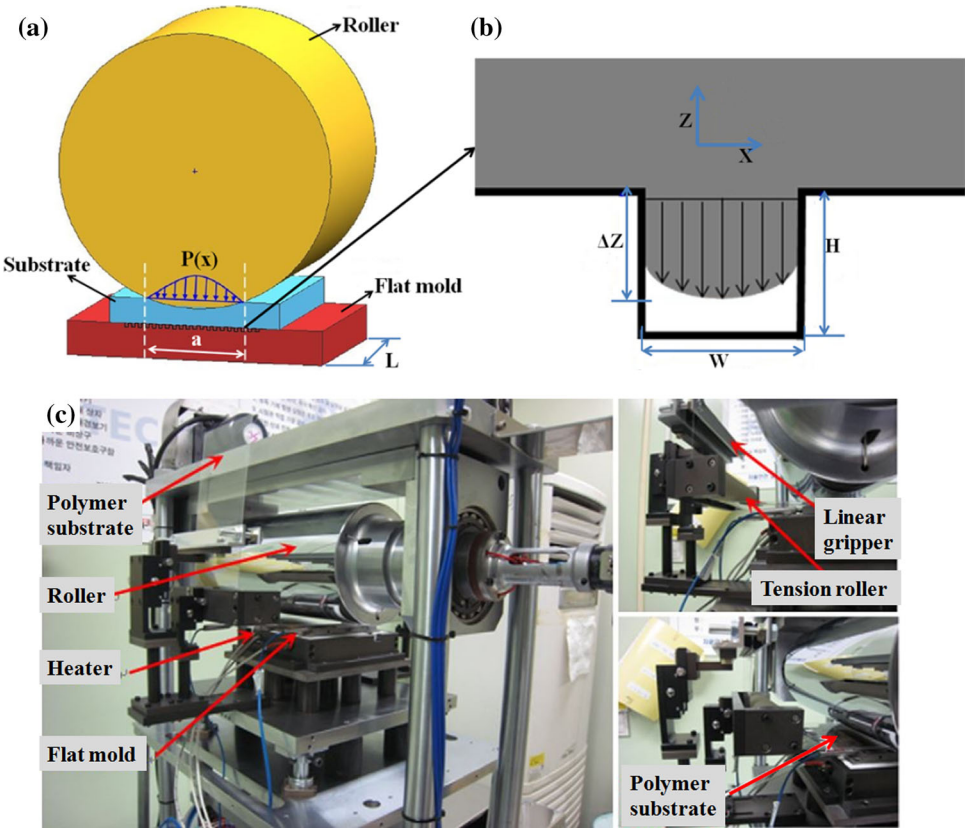

Fig. 6 **a** Geometrical configuration considered for the analytical model of roll to plate hot embossing process with flat mold, **b** Polymer flow in micro/nano size cavities on the mold during embossing, and **c** Roll to plate hot embossing setup developed by Shuhuai Lan et al. (Lan et al. 2010)

mold's micro/nano-sized cavities. According to the numerical model, at a lower value of viscosity, better replicability was expected. Since viscosity reduces with a temperature rise, better replicability was noted at higher embossing temperature values.

Recently, Jarrett J. Dumond and Hong Yee Low (2012) proposed a theoretical model for the time needed to fill the micro/nano-size cavities on the mold throughout the R2P-HE. The problem is treated as one dimensional (*1-D*) squeezing flow of the polymer substrate into extremely long micro-cavities of height (*H*) and width (*W*) shown in Fig. 7. Few assumptions were made while developing this theoretical model. The first assumption is the roller contact width (*L*), and the polymer web/workpiece thickness is substantially bigger than the height (*H*) and width (*W*) of the micro-cavities over the mold to avoid the edge and thickness effect. The second assumption is that the roller diameter is much larger than the height (*H*) and width (*W*) of micro-cavities on the mold. Hence, the roller curvature fails to influence the polymer flow behavior. The following assumption is that the pressure is uniformly distributed over the roller contact width (*L*) throughout the embossing process. Finally, the polymer substrate is considered incompressible, and polymer flow is assumed to be ideally viscous, with perfect adherence of the polymer substrate to the mold surface. Equation 2 gives the time needed to fill micro/nano-sized cavities over the mold (t_{fill}).

$$t_{fill} = \frac{6\eta(T).H^2}{P(t).W^2} \tag{2}$$

where, $\eta(T)$= viscosity of polymer substrate respective temperature, *P(t)* = time dependant applied pressure.

This proposed theoretical model does not apply to the non-uniformly distributed pressure and other shapes of the micro-patterns like a circular, square, triangle, pyramidal, etc., or any other odd-shaped micro-pattern on mold. For continuous embossing t_{fill} is less than or equal to the ratio of the roller contact width (*L*) to the polymer feed rate (*V*). The modified equation is given in Eq. 3.

$$\frac{L}{V} \geq \frac{6\eta(T).H^2}{P(t).W^2} \tag{3}$$

To find the interrelation between the polymer feed rate and the polymer substrate's viscosity, applied pressure, geometric factors, Eq. 3 is rearranged.

$$V \leq \frac{L.P(t).W^2}{6\eta(T).H^2} \tag{4}$$

The polymer feed rate equation (Eq. 4) clearly shows that at a low value of aspect ratio (*H/W*) of micro-patterns and low viscosity values of the polymer substrate, the polymer feed rate theoretically increases.

Sung-Won Youn et al. (2008) modified the existing roll-to-plate hot embossing with a flat mold set up to improve the replication rate by implementing an automatic mold releasing mechanism. The schematic and actual setup of the modified roll-to-plate (roller to plate) hot embossing setup with the mold releasing mechanism is indicated in Fig. 8a and b, respectively. This setup comprises a roller incorporated with the heating unit, a flexible mold attached to the guidepost through a supporting coil and puller, a moving platform with a heating coil, a polymer substrate, and a base plate. This automatic mold releasing system minimizes the embossed micro-pattern distortion because of shrinkage differences within the mold and polymer web/substrate. The workpiece is fixed over a moving platform, and it moves parallel to the roller while the embossing force is applied on the roller. The control system controls the speed of the moving platform and the applied force. As the roller moves forward, pullers move upward across the guidepost to automatically detach the mold from the embossed workpiece. After that, the mold comes back to its home position. Embossing was carried out on the PET (polyethylene terephthalate) and COC (cyclic olefin copolymer) film. Better replicability was observed at embossing force equal to 700 N and at embossing temperature above 50 °C of the T_g. In polyethylene terephthalate (PET) film, complete filling of micro-pattern was accomplished at roller speeds of 0.1 mm/s. With cyclic olefin copolymer (COC) film, the complete filling was obtained at roller speeds less than 2 mm/s. Using this modified setup, a light-guided plate consisting of line micro-patterns of 38 µm wide, 63 µm long, and 8.5 µm deep were fabricated for the backlight panel. The optical microscope image, *2-D*, and *3-D* profile of embossed line micro-pattern over the PET polymer substrate is shown in Fig. 8c.

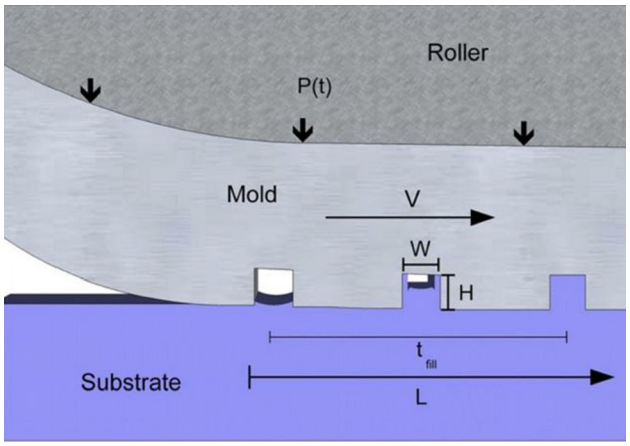

Fig. 7 One dimensional (1-D) squeezing flow of the polymer substrate into extremely long micro-channel of height (H) and width (W) (Dumond and Yee Low 2012)

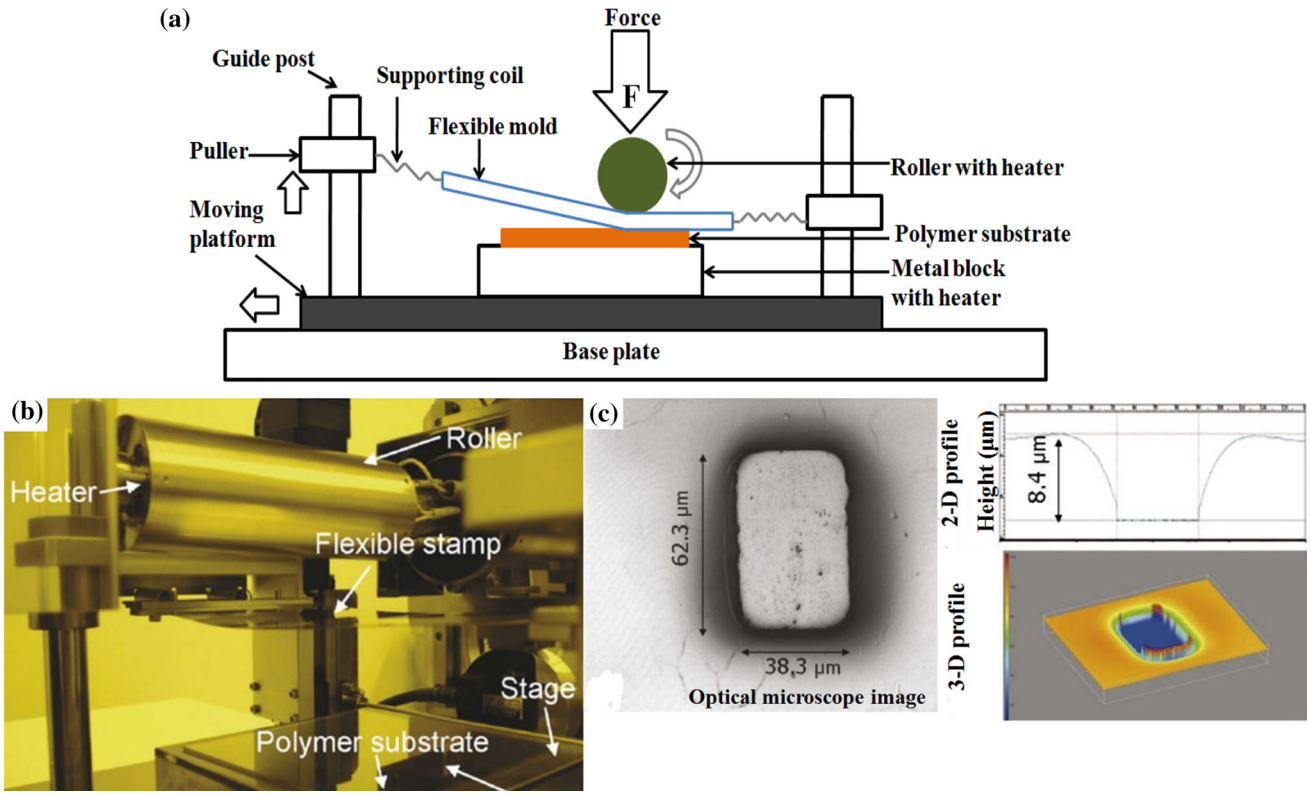

Fig. 8 Roll to plate hot embossing with automatic mold releasing mechanism- **a** Schematic setup, **b** Actual experimental setup, and **c** Optical microscope image, 2-D and 3-D profile of embossed line micro-pattern over the PET polymer substrate (Youn et al. 2008)

The setup of a roll-to-plate hot embossing was further modified by HyungJun Lim et al. (2011) who implemented a movable press roller rather than the flexible mold. The roll to plate hot embossing with movable press roller is shown in Fig. 9a. In this setup, mold is installed on a hot plate, which heats mold over the T_g of the polymer web. During the embossing stage, the press roller with flexible substrate rolls over the mold and presses the flexible substrate against the mold. Embossing is carried out through a series of line contact, and afterward, the polymer substrate is cooled by compressed air. The guide rollers also move with the press roller during embossing to prevent the shrinkage and stretching of the polymer web/workpiece. The vertical transition stage controls the upward and downward movement of the press roller. The upper and lower side springs inside the roller holder support the movable press roller and deliver the embossing force through the vertical translation stage. When the movable roller makes contact with the mold, the amount of embossing force is controlled by the stiffness of the springs inside the roller holder and the vertical movement of the translation stage.

After completing the embossing cycle, i.e. (complete movement of the movable roller from the left to right as illustrated in Fig. 9a), the movable roller with polymer workpiece moves upward and comes back to its home position. After this, the supply roller and withdrawal roller rotates to feed the new plain polymer workpiece for the next micro-pattern embossing, and the cycle is repeated. All the roller movement in the setup is controlled through a PLC (Programmable Logic Controller). The process parameters like the speed of the movable roller during the embossing stage, embossing force, hot plate temperature, and cooling requirements of the polymer workpiece significantly affect the replicability of micro-patterns over the polymer web/substrate. This capability of the setup was verified by successfully replicating micro-sized concentric circles and nano-scaled line patterns over a polycarbonate substrate. The SEM images of micron-sized concentric circles and nano-scaled line patterns embossed over the polycarbonate (PC) substrate are depicted in Fig. 9b and c, respectively. The roll to plate hot embossing setup is commercially used to fabricate flexible electronic devices like solar cells, light diffusers, bendable displays, anti-reflection films, etc.

2) Roll-to-roll hot embossing (R2R-HE)

In conventional hot embossing, the micro-patterns are replicated over a small area on the substrate. To increase productivity, R2R-HE has been developed. It is a variant of

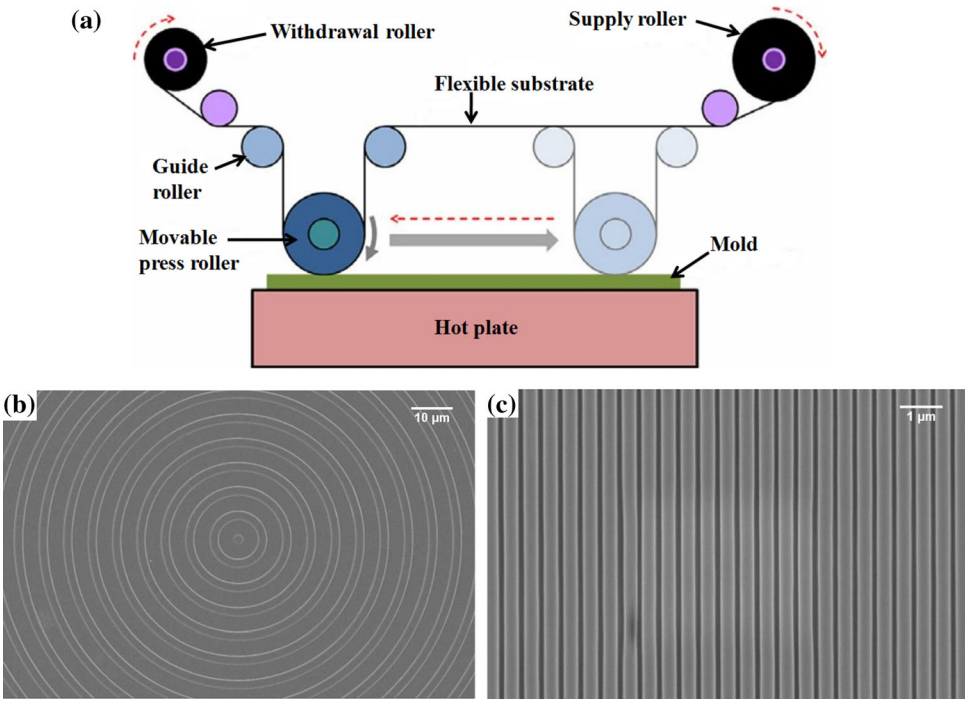

Fig. 9 **a** Roll to plate hot embossing with movable press roller, SEM images- **b** micron-sized concentric circles, and **c** nano-scaled line patterns embossed over the polycarbonate (PC) substrate (Lim et al. 2011)

R2P-HE, as explained in the preceding section. In R2R-HE, the micro-patterns can be reproduced over a large substrate area, which improves its productivity. The setup of R2R-HE is illustrated in Fig. 10a. In R2R-HE, it is tough to fabricate the micro-patterns over the entire circumference of the roller due to its circular shape. To address this, micro-patterns were manufactured over a thin film by several methods like UV-lithography followed by electroforming or electroplating process (Ishizawa et al. 2008; Shan et al. 2009), photolithography followed by wet etching process (Idei et al. 2006; Zhong and Shan 2012; Kodihalli Shivaprakash et al. 2019b), maskless photolithography followed by plasma etching (Kodihalli Shivaprakash et al. 2019a), electron beam lithography followed by the Ni-electroforming process (Habermehl et al. 2019), and that film is then wrapped around a roller called as embossing roller.

The seam on the roller surface is a recurring issue with thin mold wrapped around the embossing roller, resulting in a cyclic discontinuity in the embossed features (Lee et al. 2012). Nevertheless, there are several applications such as display or microfluidic devices where micro-pattern discontinuity is acceptable. Initially, the micro-patterns on seamless roller were developed through laser writing (Lee et al. 2009; Du et al. 2012; Rank et al. 2017; Lang et al. 2017) and the direct electron beam writing method (Taniguchi and Aratani 2009; Taniguchi et al. 2010). But these methods face severe issues like small aspect ratio, high fabrication cost, complex profile control, low throughput, and poor surface roughness. Therefore, the micro-patterns on seamless roller were developed through UV-photolithography followed by wet etching and electro-polishing to solve these issues. Before UV-photolithography, the roller was coated with a photoresist using a specially designed pneumatic airflow coating method. The ultraviolet (UV) exposure was aligned parallel to the coated roller, and its motion was precisely controlled. It helps transfer the micro-patterns over the photomask to the photoresist-covered roller (Hong-Wei Chen et al. 2010; Li et al. 2011; Huang and Lee 2013). However, this process is complex, costly, and time-taking, so it is recommended to use a seamless roller only when continuity in embossed micro-patterns is required. Otherwise, one can go ahead with the conventional embossing roller, i.e., micro-patterned film wrapped around the roller.

The sheet of polymer substrate is passed within the embossing roller as well as the supporting roller. The embossing roller is heated until its temperature exceeds the T_g of the polymer web, and load is imposed on it throughout the embossing stage. In R2R-HE, roller feed and roller temperature significantly influence the accuracy of the embossed features over the polymer workpiece (Ng and Wang 2008; Shan et al. 2008; Soh et al. 2008). In R2R-HE, contact time between the polymer workpiece and mold is short, due to which less heat is transmitted through the mold to the polymer workpiece. Preheating the polymer before embossing softens the polymer web/substrate and improves the depth of the embossed micro-patterns (Kim et al. 2015). Lip Pin Yeo et al. (2009) installed a heater in the conveyor called a preheating unit for the preheating of

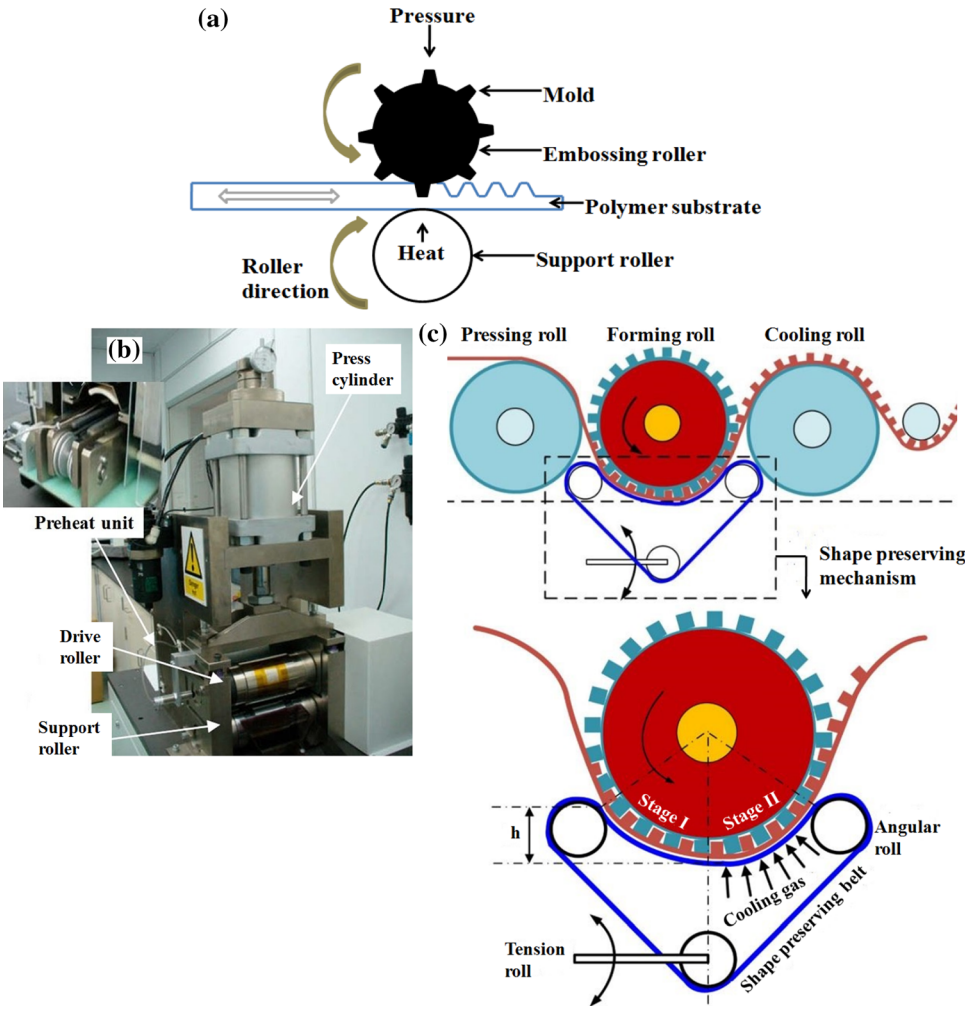

Fig. 10 **a** Roller to roller hot embossing, **b** Roll to roll hot embossing with preheating unit (Yeo et al. 2009), and **c** Roll to roll hot embossing with shape preserving mechanism (Peng et al. 2016)

the polymer substrate. The R2R-HE setup with a preheating unit is shown in Fig. 10b. Taking motivation from this, Thomas Velten et al. (2011) used heated metal plates for preheating the polymer substrate and passed the polymer substrate film through the hot metal plates before passing through the roll-to-roll embossing system. In this work, the silicon film was wrapped around the embossing roller, and micro nubs were developed on silicon film by lithography followed by a dry etching process. The micro-holes were formed on COC polymer substrate using this preheated roll-to-roll embossing system. These embossed micro-holes were utilized for cell culture purposes.

If the roller feed is more than the optimum value, the embossing is improper due to insufficient time for the transference of micro-patterns from the mold to the polymer web/ workpiece. If the embossing temperature is more than the optimum value, the polymer can become more viscoelastic, and thermal reflow might happen. During the deembossing stage, due to improper cooling polymer surface remains in a rubbery state. It tries to flatten out to minimize its surface energy. Due to this, the polymer may regain its original shape; this phenomenon is called thermal reflow. In R2R-HE, when the T_e (embossing temperature) is set 35–40 °C above T_g, the viscosity of the polymer substrate decreases rapidly, and it becomes significantly fluid. At this stage, the polymer substrate is subjected to a relaxation phase, as a result of which the embossed flat surface is drawn back by simple viscous flow to minimize the surface energy. This results in the decreased height of the embossed micro-patterns. The thermal reflow is mainly observed when deembossing is performed at high temperatures (35–40 °C beyond the T_g) without cooling. In R2R-HE, the mold temperature is constant throughout the process.

In contrast, in conventional hot embossing, the mold undergoes a heating and cooling cycle. Due to the absence of a cooling phase in an R2R-HE, embossed micro-pattern in contact with mold starts to reflow quickly as the mold and polymer substrate separate. This reflow brings down the replication quality of the replicated micro-pattern. To avoid this, it is preferable to carry out the embossing process near glass transition temperature even though

greater accuracy was observed at a temperature higher than T_g (30–40 °C above the T_g) in the case of the R2R-HE. In addition, sometimes melting of polymer web/substrate also occurs, and it sticks to the roller, resulting in deformation of the embossed micro-patterns. So it is necessary to fix the roller feed and T_e at optimum values for better accuracy of the embossed micro-structure (Yeo et al. 2009).

Micro-patterns were successfully embossed on textile fibers employing R2R-HE (Schift et al. 2006). The optimization was carried out using the design of experiments (Box–Benhken design matrix) to optimize the operating parameters in the R2R-HE. For the optimization, embossing pressure, roller temperature, preheat temperature were considered, as well as the normalized depth of embossed micro-patterns over the PMMA workpiece/substrate was investigated. The outcome of experimentation confirms that at higher T_e, a decrement in the depth of embossed micro-patterns was observed. This decrement in depth occurs mainly due to the thermal reflow mechanism. The best or optimum result was achieved at T_e of 110 °C (nearer to T_g), P_e of 6 bar, and preheat temperature of 105 °C. Micro-mixer was fabricated on PMMA substrate using these optimum parameters. The performance of the fabricated micro-mixer was characterized by conducting the fluid flow test. This test shows that the complete mixing of the solution took place in the embossed micro-mixer (Yeo et al. 2010).

Yujun Deng et al. (2014) fabricated micro-pyramid patterns over polyvinyl chloride (PVC) film using R2R-HE. A central composite design was applied to investigate process parameters systematically, and an empirical model was developed. In this work, embossing temperature, applied load, and feeding speed of the polymer substrate were considered as input parameters. The RSM (response surface methodology) was implemented to optimize parameters for achieving 100% replication accuracy. This optimization shows that when the process parameters are set at optimum values, a replication accuracy of 94% was achieved. The PMMA and COC polymer substrate have superior physical and chemical properties. The PMMA substrate has a low hydrophobicity and good optical transparency. In contrast, COC polymer substrate is biocompatible, has a high resistance to a chemical reaction, and excellent optical clarity (near-visible and ultraviolet range). By taking advantage of these properties and mass manufacturing capability of the R2R-HE, Metwally et al. (2012) and Tsao et al. (2012) fabricated a microfluidic chip.

Sahil et al. (2009) developed a 3D-numerical model considering the linear viscosity of the polymer substrate for R2R-HE. They investigated the polymer flow during the embossing stage at a constant temperature. The filling rate was investigated for various micro-cavities like circular, triangular, etc., with a 2-D numerical model (Sahli et al. 2010). It is noted that the filling time of semicircular cavities was significantly more than the triangular cavities because of the volume difference.

Recently, Yujun Deng et al. (2015) validated this 3D numerical model to fabricate micro-pyramid patterns over the polymer web/substrate (PVC film). In this work, they investigated polymer flow throughout the embossing and deembossing stage during an R2R-HE process. It was pointed out that the temperature gradient in the path of the thickness softens the embossing area and makes sure that micro-patterns are well replicated on the polymer substrate throughout the R2R-HE. During the embossing stage, the edges of the mold compress the polymer substrate and extrude it along the sidewalls of the mold. The creep strain (ε^c) is much temperature-responsive as compared to the instantaneous elastic strain (ε^o). The creep strain (ε^c) starts to grow after a particular time interval as temperature goes beyond the specific value. This creep strain primarily occurs at the top surface of the polymer web due to high local temperatures. Recovery in the height of replicated micro-pyramid shape patterns were observed after deembossing, which can be controlled by implementing the cooling process throughout the demolding stage to attain excellent embossing accuracy.

The pile-up type of defect is also observed in the embossed part in case of R2R-HE. This pile-up type of defect is minimized by the setting process parameters like T_e and P_e at higher value (Zhong et al. 2015). In R2R-HE, different defects like bubble defects, platform, and collapse-like defects were noticed in the embossed micro-patterns (Yi et al. 2015). The different types of defects in embossed micro-pyramid patterns are indicated in Fig. 11. To figure out the main reasons for these defects, Jin Wang et al. (2015) developed a 3-D FEA model based on the Maxwell model. In this model, the polymer workpiece/web was treated as a viscoelastic material. This simulation shows that platform type defect appears by means of adverse embossing conditions like low embossing pressure, which restricts the polymer flow during embossing. The bubble type of defect primarily occurred at a high value of T_e and feeding speed. At high values of embossing temperature and feeding speed, polymer material flows along the sidewall of the mold. As a result, it is deformed into the two peak mode/ concave shapes (shallow at center and peaks at the corner). Finally, the collapse type of defect occurs by means of the rapid recovery of the polymer substrate after the deembossing stage.

The same research group proposed that it is necessary to implement quick cooling for minimizing such types of defects, and a system with longer holding is required. To achieve this, the shape-preserving mechanism was implemented in the R2R-HE. The shape-preserving mechanism

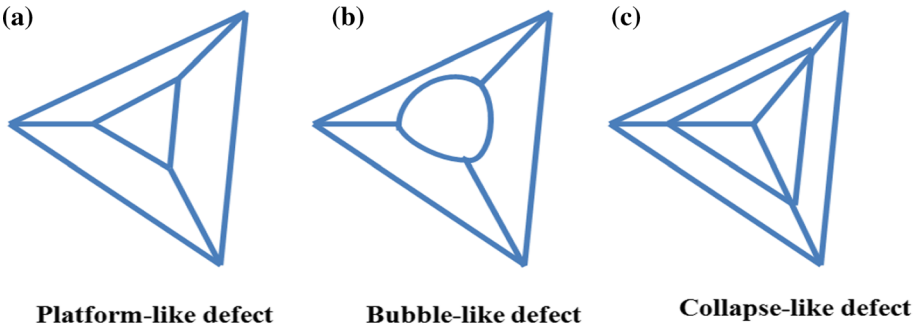

Fig. 11 Different types of defects in embossed micro-pyramid patterns

(SPM) is shown in Fig. 10c. This mechanism comprises the shape-preserving belt (SPB), tension roller, two angular rollers, and a cooling gas nozzle. During the working cycle (in step one), the shape-preserving belt (SPB) presses the structured substrate against the hot embossing roller. Because of this, the polymer substrate keeps flowing into the micro-cavities on the embossing roller. In stage two, cooling gas cools down the shape-preserving belt (SPB) and micro-patterned substrate immediately. This cooling gas cools the embossed substrate below the T_g of the substrate.

Consequently, it efficiently reduces the flow-back of the polymer material after the deembossing stage. The influences of the tension force (TF) as well as wrap angle (WA) concerned with the SPM (shape-preserving mechanism) were investigated systematic way. The experiment outcomes show that a maximum value of tension results in high P_e, and a greater wrap angle leads to long-lasting flow. So better replication accuracy was achieved at a higher value of tension force and wrap angle (Peng et al. 2016).

Nagato et al. (2010) designed and developed a setup to fabricate multi-layered nanogaps and nanostructures over the polymer substrate. The setup developed by Nagato et al. (2010) is indicated in Fig. 12a. In this setup, roller hot embossing is combined with the bonding process to fabricate the multilayer nanogaps and nanostructures. The thin PMMA film is deposited over the silicone rubber film, acting as a backup film. The embossing was carried out using a roller mold with nano-scale features and a featureless roller with plain mold. Better results were achieved in the featureless roller with plain mold. The embossed sheet is cooled with Nickel mold until the temperature goes down below the T_g and then separated out. Therefore due to proper cooling no viscoelastic recovery could happen. Better embossing and bonding result was observed at T_e = 145 °C, P_e = 1Mpa, bonding temperature = 100 °C and observed feed rate = 0.6 m/minute. The SEM image of multilayer nanogaps with fiver-layer nano-scaled pattern is shown in Fig. 12b. For the fabrication of multilayer nanostructures shown in Fig. 12c initially the polymer film is embossed through the thermal assisted roller embossing by using plain mold. Then chromium of 25 micron thickness is sputtered over the embossed surface. Next the plain mold is rotated through the 90° and roller embossing has been carried out. In this way multilayer nanostructures were fabricated over the PMMA substrate.

4 Current innovations in roll-to-plate hot embossing (R2P-HE) and roll-to-roll hot embossing (R2R-HE)

4.1 Rapid manufacturing of UV curable micro-patterns on glass or polymer substrate by ultraviolet (UV) assisted roll-to-plate hot embossing

There are few major issues in the conventional R2R-HE system that directly affects the replicated micro-patterns quality. When the temperature of the embossing roller is 35–40 °C exceeding than T_g of the polymer web/substrate, the polymer film significantly softens during embossing. As already explained, due to the absence of the cooling process in the deembossing stage, it undergoes a thermal reflow mechanism. As a result, the embossed micro-patterns undergo unnecessary viscoelastic recovery after the deembossing stage. Thus, it distorts the replication quality of embossed micro-patterns. In ultraviolet (UV) assisted roll-to-plate hot embossing (R2P-HE), a similar problem occurs if curable resin fails to cure appropriately before leaving the embossing roller. Thus, it is necessary to set the speed of the embossing roller and the intensity of the UV source at an optimum value (Chan-Park and Neo 2003).

For rapid production of micro-lenses over the polymer web/substrate, Chih-Yuan Chang et al. (2007) suggested ultraviolet (UV) assisted soft R2P-HE process. In this, the embossing was done at room temperature, so lower residual stresses (σ_0) were present in the replicated micro-patterns in contrast to conventional R2R-HE. In this process, the soft silicone cylinder was used instead of a metallic roller. To develop micro-cavities on silicone roller, the embossed micro-lenses array on thin polycarbonate (PC)

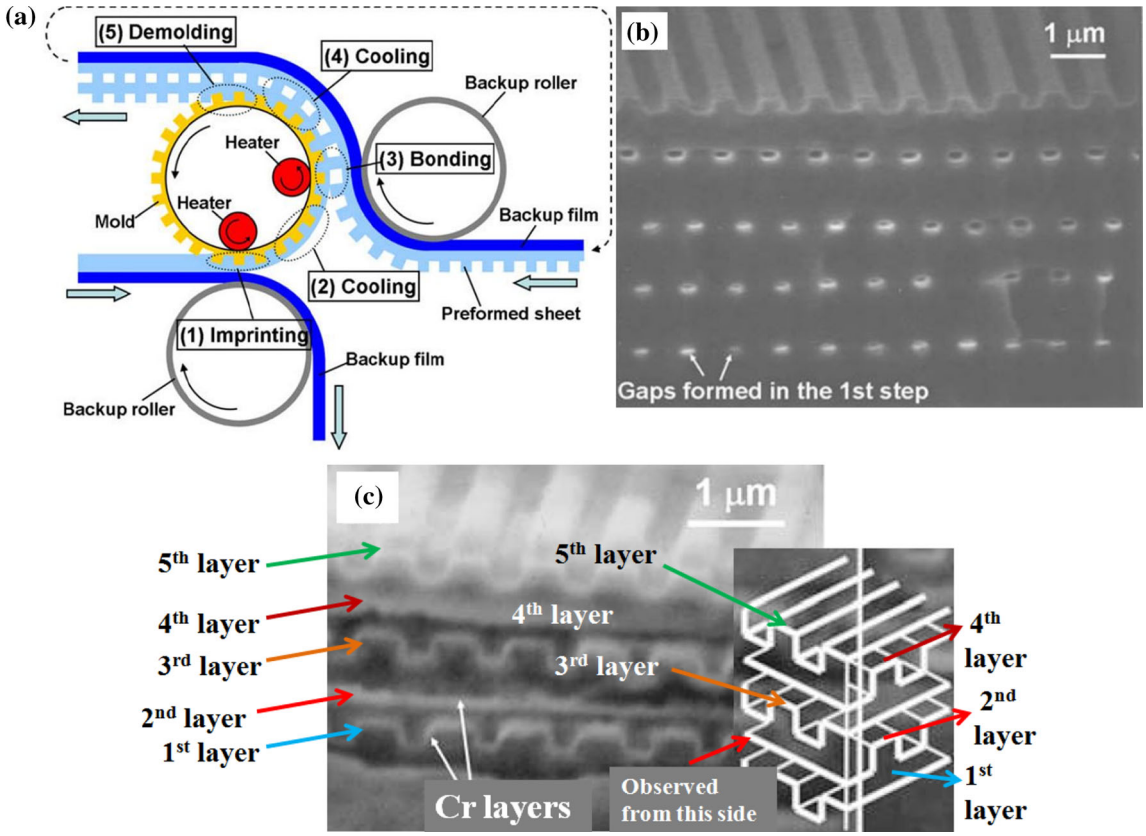

Fig. 12 **a** Roll to roll hot embossing setup developed by Nagato et al. to fabricate the multi-layered nanogaps and nanostructures, **b** SEM image of the multilayered nanogaps with five layered nanostructures, and **c** SEM image of cross section of five-layered Chromium film nanostructures fabricated by rotating the mold 90° before every embossing stage (Nagato et al. 2010)

film of 180 μm thickness was fabricated through gas-pressurized hot embossing was then wrapped around the soft silicone roller. Next, the viscous polydimethylsiloxane (PDMS) solution was poured into a cavity of a cylinder to fabricate the micro-cavities on a cylinder. Finally, this thin polycarbonate (PC) film was peeled off, and micro-cavities were developed on the silicone cylinder. The detailed procedure for manufacturing micro-cavities over the cylinder is shown in Fig. 13a. The ultraviolet (UV) assisted soft roll-to-plate embossing setup consists of a soft silicone cylinder with pressure unit (pneumatic cylinder), PMMA substrate, movable platform, ultraviolet (UV) curable polymer resin, slit die mechanism for coating of UV curable resin over the micro-cavities on the silicone cylinder, scraper to remove the excess material from the micro-cavities, and a UV lamp. The ultraviolet (UV) assisted soft roll to plate embossing setup is shown in Fig. 13b.

As already mentioned in R2R-HE, embossing pressure and roller speed significantly impact the replicability of the embossed/replicated micro-patterns. In this experimentation, embossing pressure (P_e) was varied from 0.2 to 0.8 kgf/cm^2, roller speed from 0.65 to 1.7 mm/s, and percentage deviation in diameter, sag height of embossed micro-lenses were investigated. With P_e higher than 0.8 kgf/cm^2, distortions of the embossed micro-lenses were observed. If roller speed is more than 1.7 mm/s, the ultraviolet (UV) curable polymer resins do not adequately adhere to the roller. Due to insufficient time, it is not sufficiently cured on the polymethyl methacrylate (PMMA) polymer substrate. If the roller speed is less than 0.65 mm/s, excessive curing occurs and results in distortion and shrinkages in the embossed micro-lenses. The R_a (surface roughness) and optical characteristics of embossed micro-lenses were assessed through atomic force microscopy and beam profiler, respectively. Surface roughness (R_a) of the embossed micro-lenses was noted over a 5 μm × 5 μm area and found to be 8.36 nm. The SEM image and surface profile of embossed micro-lenses over polymer substrate through UV-assisted R2P-HE is shown in Fig. 13c. The normalized intensity of embossed micro-lenses was distributed uniformly. The ultraviolet (UV) assisted R2P-HE effectively supports the large-scale fabrication of micro-lenses over a polymer web/substrate at a cheap cost. With the help of this setup, micro-patterns were also developed on the glass substrate (Liu and Chang 2007).

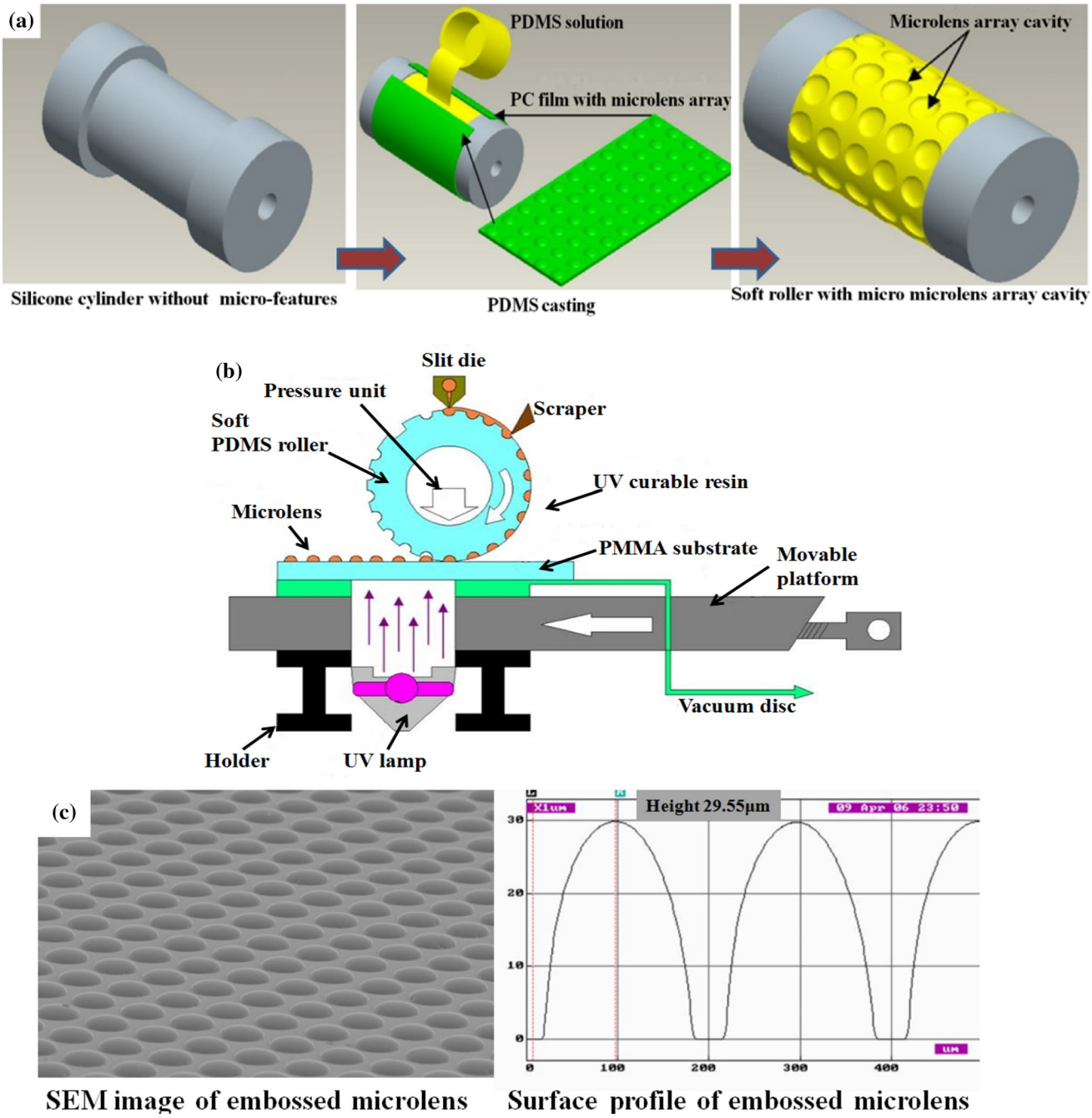

Fig. 13 **a** Detailed procedure for the manufacturing of micro-cavities over the cylinder, **b** Ultraviolet (UV) assisted soft roll to plate embossing setup, and **c** SEM image and surface profile of embossed micro-lenses over polymer substrate through UV-assisted R2P-HE (Chang et al. 2007)

To fabricate a set of micro-lenses on a glass workpiece, Chang et al. (2006b) replaced the silicone roller with a steel roller in the ultraviolet (UV) assisted roll-to-plate hot embossing setup. The embossed micro-lens array on polycarbonate (PC) workpiece by gas-pressurized hot embossing was used to manufacture the nickel mold. For the development of nickel mold, 100 nm thick silver film was deposited on the embossed micro-lenses followed by the Ni-electroforming process. As a consequence that, 0.3 mm thick nickel mold with micro-cavities was prepared. Later this Ni-mold was wrapped around the steel cylinder, and the cylinder was pressed against the glass workpiece. The sets of micro-lenses were developed on a glass workpiece and cured through UV radiation at room temperature. This manufacturing process is a mass-manufacturing approach suitable for manufacturing micro-lenses on glass workpieces. Although, micro-cavities on nickel

mold through Ni-electroforming is a complicated, prolonged and costly process.

To manufacture micro-lenses on a glass substrate, Chia-Nying Hu et al. (2011) developed an ultraviolet (UV)-assisted two wheels roll-to-plate hot embossing setup. One roller was used to emboss micro-lenses over a substrate, and the other roller was used to separate the mold from the UV-cured micro-lenses. The setup of UV-assisted two wheels roll-to-plate hot embossing (R2P-HE) is shown in Fig. 14. This setup consists of two steel rollers, conveyor type mold made of polydimethylsiloxane (PDMS) material, UV curable resin, glass substrate, and ultraviolet (UV) lamp. In this setup conveyor mold of polydimethylsiloxane (PDMS) material was wrapped around the two cylinders. To fabricate polydimethylsiloxane (PDMS) mold at the start, the photoresist was spin-coated over the Si-wafer. Micro-cylindrical patterns were developed on the silicon (Si)-wafer with the photolithography process. These micro-cylindrical patterns were then transformed into micro-lenses through the thermal reflow method. Next, polydimethylsiloxane was spin-coated on these micro-lenses, followed by the baking process. Finally, polydimethylsiloxane film was scratched off from the mold. This polydimethylsiloxane mold was then wrapped around the two cylinders. Finally, the UV-curable resin was spin-coated over the glass workpiece. In this work, the impact of ultraviolet lamp exposure time and rolling pressure on the replicability of micro-lenses were examined. The result confirms that if UV light exposure goes beyond the optimum value, it does not majorly affect the quality of embossed micro-lenses. But if the rolling pressure is set at a higher value, then deformation in the polydimethylsiloxane mold occurs. While at lower values of rolling pressure, the mold filling is incomplete. The best replication result was observed at a rolling pressure of 200 N/cm^2 and UV lamp exposure time of 4 min.

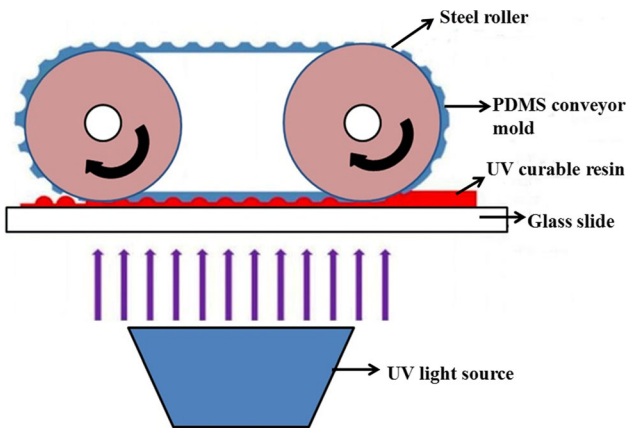

Fig. 14 UV-assisted two wheels roll to plate hot embossing

Ting et al. (2008b) fabricated conical, cylindrical arrays over a polymer substrate to simulate the anti-reflection film with UV roller embossing. The mold consists of a nano-scaled pattern manufactured through the Ni-electroforming process and wrapped around the roller in this setup. Anti-stick coating was applied over the roller mold for quickly releasing the mold during the deembossing phase. The embossed nano-scaled conical cylinder array has an average diameter (d_{avg}) of 200 nm, an average height (h_{avg}) of 350 nm, and a pitch of 200 nm. The reflectance was achieved is 2.45%, and transmittance is above 90%

Initially, the primary focus was on the impact of operating parameters on accuracy as well as the quality of replicated micro-patterns by UV-assisted roller embossing. Lesser priority was given to the effects of the surface energy ($E_{Surface}$) of mold and the shape and directions of micro-patterns on embossing roller over replicated micro-patterns replication quality and accuracy. Osamu Nezuka et al. (2008) investigated these operating parameters and their influences on embossed micro-patterns. In this work, a V-groove patterned nickel mold coated with trimethoxysilane was used. The contact angle was measured after coating, and it was confirmed that the coating lowers the surface energy ($E_{Surface}$) of the mold. As a result, the substrate was quickly released from a mold after embossing without influencing the accuracy of the micro-patterns. Embossing was carried out by wrapping the mold over the roller in two ways—in first, the grooves were parallel to the rolling orientation, and in second, the grooves were transverse to the rolling direction. With parallel grooves, tearing was observed during the deembossing, and it damages the sharp edges of the V-shape groove. While grooves in a transverse direction, the sharp edges of the V-groove were observed, but biting traces were noted over a sidewall of the grooves. These traces are due to mechanical interaction between the replicated micro-patterns and V-grooves over the mold. It was concluded that it is preferable to perform embossing by arranging mold so that grooves are transverse to the rolling direction.

4.2 Hybrid extrusion roll-to-roll hot embossing (hybrid extrusion R2R-HE)

In this type, the extruded polymer film is immediately passed through the R2R-HE setup (Jiang et al. 2007; Chang and Tsai 2015; Chang and Hu 2018). The schematic and actual setup of hybrid extrusion R2R-HE setup is indicated in Fig. 15a and b, respectively. Liang-Ting Jiang et al. (2007) developed this setup by integrating the roll-to-roll hot embossing set up with the single screw extrusion setup. First, Micro-lenses were developed on polycarbonate film using this setup. Then, the micro-patterns were directly

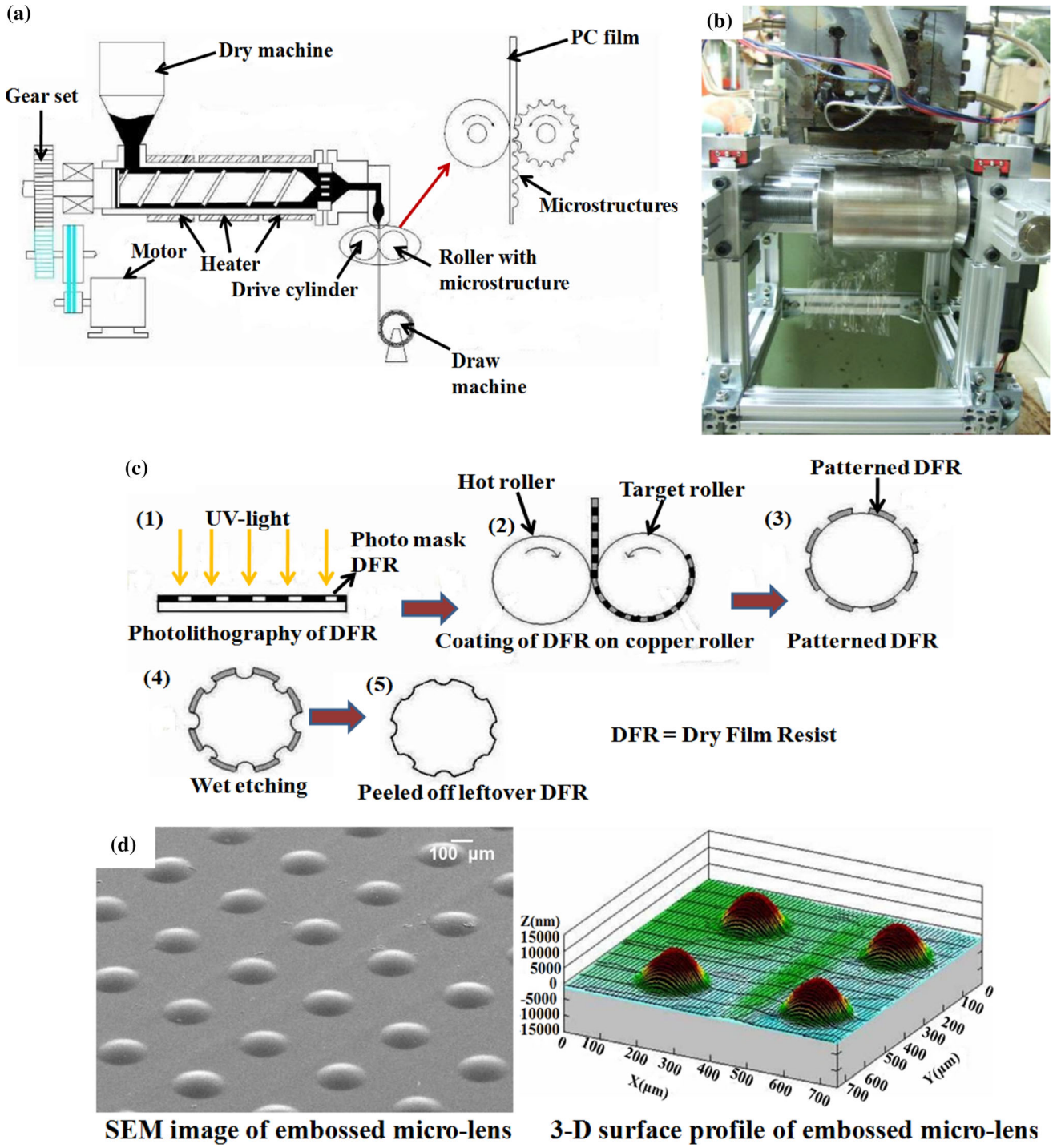

Fig. 15 **a** Schematic setup, **b** Actual setup of hybrid extrusion roll to roll hot embossing setup, **c** Step by step process for fabrication of embossing roller, and **d** SEM image and 3-D surface profile of embossed micro-lenses (Jiang et al. 2007)

manufactured on a copper roller using dry film resists (DFR). Finally, this micro-patterned copper roller was used as an embossing roller. The stepwise process for the fabrication of the embossing roller is shown in Fig. 15c.

Initially, micro-holes were developed on the dry film resist through photolithography. This DFR (dry film resist) was then coated around the copper roller by heating and applying suitable pressure. Further micro-holes were developed on copper roller through a wet etching process. This embossing roller is used in the embossing setup below the slit-die of the extrusion process. During the process, the extruded hot polycarbonate sheet was immediately passed

through the embossing setup. The drive roller pressed the hot polycarbonate (PC) film against the embossing roller, which partially fills the micro-holes on the embossing roller based upon the combined action of surface tension and P_e. Thus a (200 × 200) convex micro-lens array was developed on polycarbonate (PC) film. The SEM image and 3-D surface profile of embossed micro-lenses is depicted in Fig. 15d. In traditional hot embossing and R2R-HE, the polymer film used as a substrate is manufactured through the extrusion process only. But during embossing, the polymer is reheated, and during deembossing, it is cooled. But in this process, the hot extruded film is embossed immediately after its extrusion. As a result, low thermal stresses are developed in the embossed micro-patterns, and it also helps improve thermal stability.

This setup was further utilized by Tzu-Chien Huang et al. (2008) to fabricate a plastic diffuser. To improve the performance of plastic diffusers, this setup combines the surface-relief and particle-diffusing functions. The extruded composite film (PC/diffusion beds) was immediately passed through the R2R-HE setup. The micro-patterns were produced over the embossing roller by turning process using a tool having a nose radius of 400 µm. These micro-patterns were replicated on the extruded composite film at the optimum condition of working parameters. In this work, extrusion dies temperature, P_e, and roller speed were considered, and their impact on the height (h) of embossed micro-patterns at the center and its side area was investigated. A Haze meter was used to measure the total and diffuse transmittance at different conditions. The diffusing result of laser light at other conditions is shown in Fig. 16. The maximum diffuse transmittance, i.e., 87.7%, was noted in a composite film with embossed micro-patterns.

4.3 Double-sided roll-to-roll hot embossing (double-sided R2R-HE)

For achieving the commercial targets, it is necessary to fabricate the product with high volume and rapid manufacturing methods. Furthermore, for increasing the embossing rate in R2R-HE, there is a necessity for embossing on both sides of the polymer substrate in one cycle. Considering this, Tapio Makela et al. (2008) developed a double-sided R2R-HE setup. They proposed two approaches for the double-sided R2R-HE. The initial one is the sequential double-sided R2R-HE, and the second one is the simultaneous R2R-HE system. The setup of the sequential double-sided R2R-HE is illustrated in Fig. 17a.

In the sequential double-sided R2R-HE system at the first stage, the top face of the polymer gets embossed, followed by embossing at the bottom face of the polymer web within the same embossing cycle. A 100 µm thick micro-structured nickel master was wrapped around the roller, placed at the top and bottom surface of the polymer web/workpiece as shown in Fig. 17a; these rollers are called embossing roller. The backing roller is there for support, but these rollers are unstructured and elastic. In

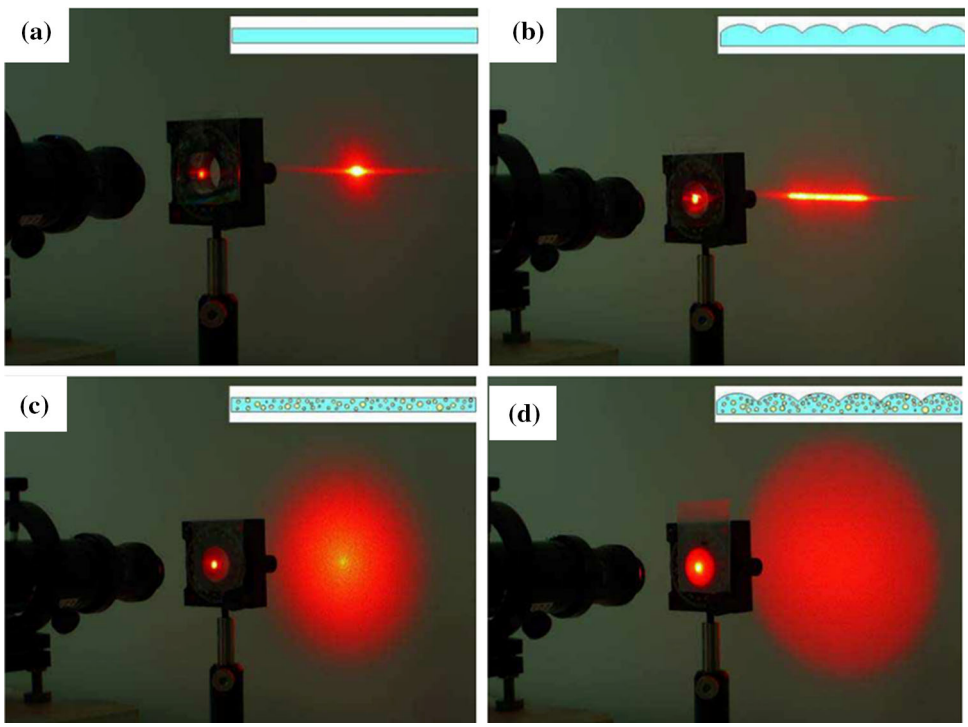

Fig. 16 Diffusing result of laser light at different conditions- **a** A flat polycarbonate (PC) substrate, **b** A PC substrate with embossed micro-patterns, **c** A flat PC/ diffusion beads composite film, and **d** A PC/ diffusion beads composite film with embossed micro-patterns (Huang et al. 2008)

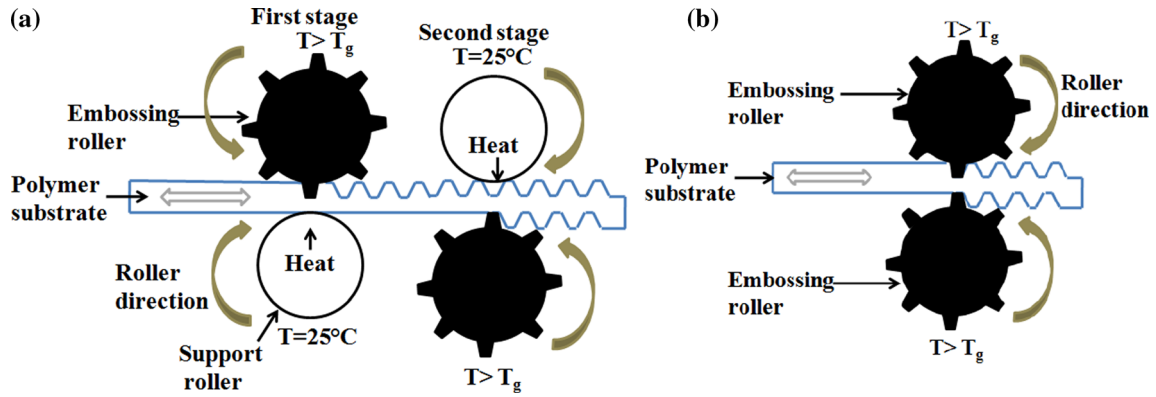

Fig. 17 **a** Sequential double-sided roll to roll hot embossing, and **b** Simultaneous double-sided roll to roll hot embossing

this work, cellulose acetate film (T_g = 120 °C) was used as an embossing substrate. In this setup, both the embossing roller was heated near T_g of the polymer substrate by placing an electric heater inside the roller. The backing roller is set at 25 °C, enhancing the contact area between the two rollers. The contact length between the rollers is 5 mm, corresponding to an embossing time of 1.6 s. No separate cooling unit is required in this system. The best embossing was achieved by trial and error method at a P_e and embossing speed of 8 MPa and 0.5 m/min, respectively.

In a simultaneous R2R-HE system, the embossing was done simultaneously on both sides of the polymer substrate. The setup of an accompanying double-sided R2R-HE setup is shown in Fig. 17b. Both rollers are metallic, and a structured nickel master was wrapped around both rollers. The upper roller is heated with an electrical heater placed inside the rolls, and the lower roller is heated with a hot air dryer. Both rollers were maintained at a temperature of 105 °C. The contact length between both rollers is 1 mm, corresponding to an embossing time of 0.3 s at a roller speed of 0.5 m/min. This nickel master consists of 1 µm size dot structures with 1 µm spacing. The height of these dot structures varies between 200 to 250 nm.

This work shows that in sequential embossing, proper replication was observed after the first stage of embossing. But the second stage influences the embossed micro-patterns on the upper surface of the polymer workpiece. When these embossed micro-patterns were pressed against the backing rollers in the second stage, the heights of embossed micro-dots on the upper surface were drastically reduced. While in simultaneous hot embossing, micro-patterns were embossed on both faces of the workpiece simultaneously. So there no change in the heights of micro-patterns after the embossing process. Finally, it is recommended to use the simultaneous double-sided-R2R-HE set up to fulfill the commercial targets.

4.4 Infrared (IR) assisted double-sided roll-to-roll hot embossing

In the previous studies, an electrical heater was installed inside the roller for heating purposes. In contrast, an infrared (IR) heater was fitted above and below the top and bottom roller surface in this setup, respectively. Thus, simply the surface of the roller was heated by the infrared radiation instead of heating the complete roller. It also minimizes the total cycle time. The schematic of the setup and the close-up view of the infrared (IR) assisted double-sided R2R-HE process are depicted in Fig. 18a and b, respectively.

In this work, PET (polyethylene terephthalate) and PC (polycarbonate) films were used as a substrate. The V-shaped micro-patterns of different depths, i.e., 150 µm and 20 µm, were fabricated on the roller surface by micro-electric discharge machining and diamond turning processes. Four different sizes of micro-patterns were replicated on both faces of the workpiece (indicated as 20/0, 150/0, 20/150, 150/150 for the top/bottom embossed micro-pattern sizes). The dimensions of the embossed micro-features were inspected by an optical microscope, surface profiler, and profile projector, respectively. The SEM image of the micro-pattern over roller is shown in Fig. 18c. During the embossing process, the polymer workpiece touches both rollers. The top and bottom roller are pressed against the workpiece through the pneumatic cylinder, placed at the top side of the setup. The influences of operating parameters, i.e., P_e, roller temperature, and roller speed, on replicability were investigated. It is observed that the embossed micro-patterns on the upper surface of the polymer workpiece show excellent replicability compared to the bottom surface. However, it might own to the fact that the embossing pressure was applied over the top roller. To overcome this issue, the temperature of the lower roller is fixed at a higher point than the temperature of the upper roller. Suppose the roller temperature

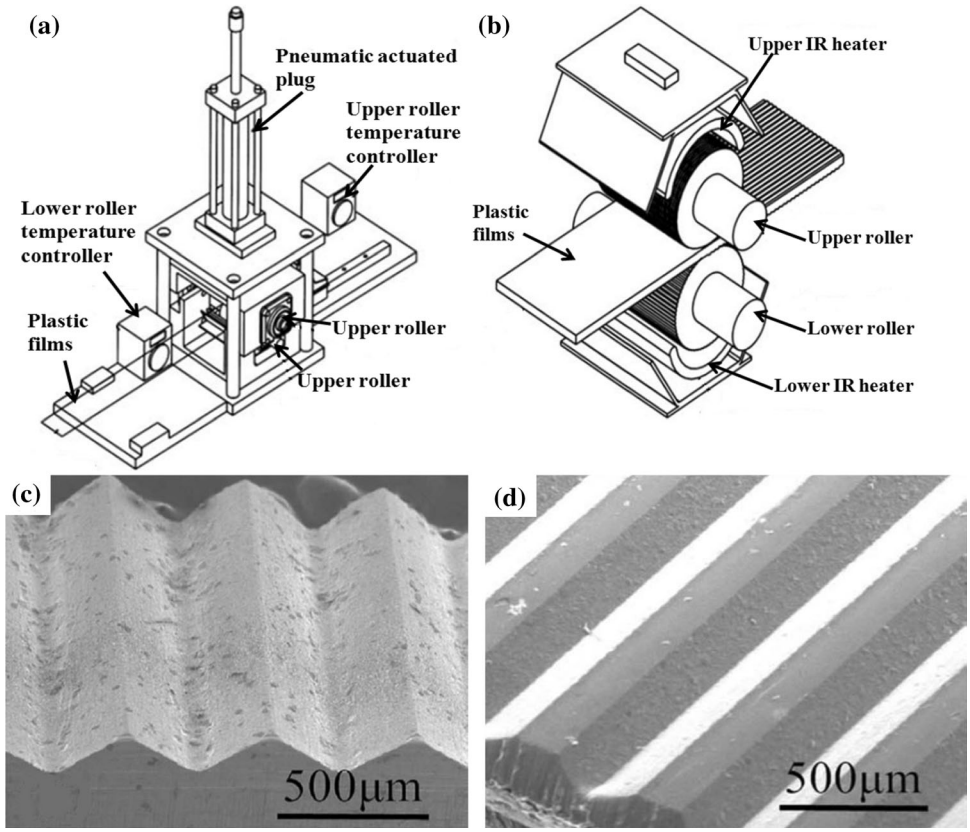

Fig. 18 **a** Schematic setup of infrared (IR) assisted double-sided roll to roll hot embossing, **b** Close-up view of infrared assisted double-sided roll to roll hot embossing, **c** SEM image of micro-pattern over roller, and **d** SEM image of embossed micro-pattern over the polymer substrate at optimum condition (Liu et al. 2012)

is fixing at a too high value. In that case, the polymer substrate enters into a fluid state, leading to reflowing the polymer material after the deembossing stage. The replicability was found to increase with embossing pressure and decrease with the speed of the roller. The SEM image of the embossed micro-pattern over the polymer substrate at optimum condition is depicted in Fig. 18d. This method effectively fabricates optical components at a cheap cost and high throughput (Liu et al. 2012).

Shih-Jung Liu et al. (2012) fabricated nano-scaled patterns on both sides of the PET (polyethylene terephthalate) film of 60 μm thicknesses based on this approach. It acts as an anti-reflection layer implemented in solar cells for performance improvement. The result shows that this nano-patterned film efficiently decreases the reflection to 4.4% from 7.4% in the wavelength range of 300 nm to 700 nm and enhances solar cell's conversion capability.

4.5 Inductive aided roll-to-roll hot embossing (inductive R2R-HE)

In R2R-HE, polymer substrate passes through the heated embossing roller and supporting roller. Through the embossing step, all the heat from the embossing roller is transmitted to the polymer web/workpiece. Due to the continuous process, it is challenging to cool the embossed film or extract such a massive amount of heat through one cycle. So it is necessary to implement a mold, which is heated and cooled within a short interval of time. So it is essential to heat the surface of the mold instead of heating the entire mold. It can be achieved with the help of induction heating. In this case, a high heating rate (more than the 100 °C/s) can be attained (Yao et al. 2006; Kim et al. 2007; Eom and Park 2009; Kimerling et al. 2009).

This induction heating module was implemented in R2R-HE. The schematic and actual setup of the inductive aided R2R-HE is illustrated in Fig. 19a and b, respectively. In this setup, electroformed micro and nano-patterned nickel molds were developed and wrapped around the embossing roller and idle roller. The conveyor mold was passed within the induction coil instead of being placed over it. The surface area of mold was increased by having longer mold. The mold was also exposed to both sides during its separation from the embossing roller indicated in Fig. 19a. Consequently, the rate of heat transfer was increased through external forced convection. The PET (polyethylene terephthalate) layer of 0.2 mm thick was used as the substrate in this work. The preheating of the substrate was carried out through the UV system. The conveyor mold target temperature (T_{Target}) was achieved by setting the induction heater power and roller speed at an optimum value. To check the potential of this setup, two

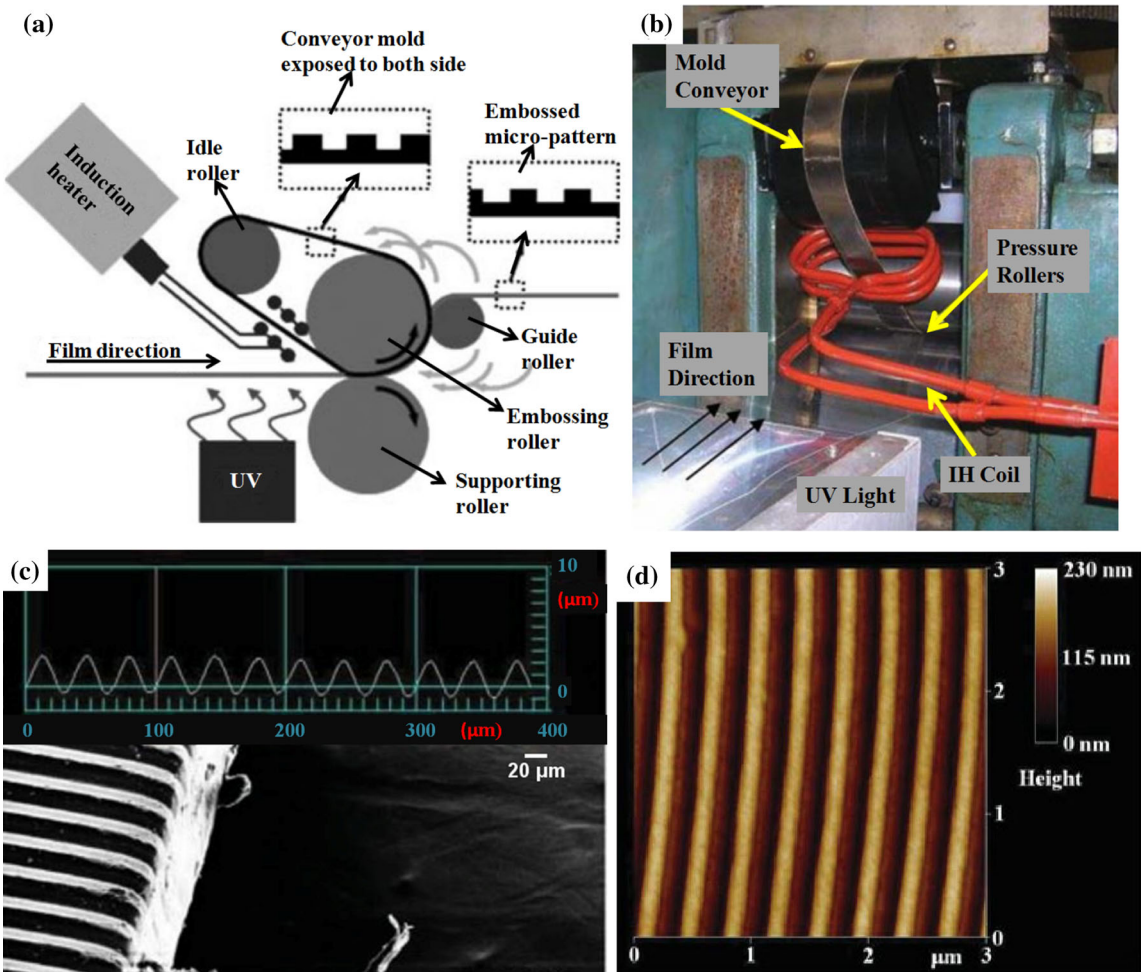

Fig. 19 **a** Schematic setup of the inductive roll to roll hot embossing, **b** Actual setup of the inductive roll to roll hot embossing, **c** SEM image of micron-sized pattern (30 μm) in length, and **d** AFM image of nano-sized pattern having 250 nm linewidth, 375 nm periods, and 200 nm height embossed over PET substrate (Fagan et al. 2009)

electroformed nickel molds consisting of micro-sized (30 μm) and nano-sized (250 nm) patterns were reproduced over the PET (polyethylene terephthalate) web/workpiece. These micro/nano-scaled patterns over the conveyor mold were well replicated on the PET (polyethylene terephthalate) film at a mold temperature equal to 250 °*C*. The SEM image of micron-sized pattern (30 μm) in length and AFM image of nano-sized pattern having 250 nm linewidth, 375 nm periods, and 200 nm height embossed over PET substrate is shown in Fig. 19c and d, respectively (Fagan et al. 2009).

Furthermore, for the uniform heating of the embossing roller surface, Yun et al. (2012) fitted the inductive heating coil inside the embossing roller. This uniform heating promotes better precision and repeatability of embossed micro-patterns. The structural analysis of the embossing roller with an inductive coil was carried out by FEA (finite element analysis) to examine the maximum stresses and deflection developed throughout the embossing step. The outcome of structural analysis confirms that the induced stress is less than yield stresses, and an inductively heated embossing roller is safe from a structural strength point of view. The electromagnetic analysis was carried out to design the inductive heating coil. The roller temperature was estimated at the center and 50 mm apart from the roller center via a thermocouple and data acquisition system. It is noted that saturation time, i.e. (time for stabilization of temperature) equals 25 s to reach the temperature of 200 °C. The micro-patterns were fabricated on the embossing roller along length direction by electroforming and engraving process. During fabrication of mold through electroforming, undercutting takes place. After the experimentation, it is observed that the width of the embossed micro-patterns is larger than the width of the electroformed mold because of the undercut phenomenon. In contrast, width is narrower in the case of engraved mold due to the capillary phenomenon. Therefore, it is preferable

to use electroformed mold than engraving mold to attain better precision and replication accuracy.

4.6 Ultraviolet (UV)-assisted gasbag roll-to-plate hot embossing

To get better pressure uniformity during the embossing stage and improve the precision of the embossed micro-patterns, an ultraviolet (UV)-assisted gasbag roll-to-plate embossing setup was developed. The schematic of the ultraviolet (UV)-assisted gasbag roll-to-plate hot embossing setup is depicted in Fig. 20a. This setup consists of a moving platform, ultraviolet curable resin, belt type mold of polydimethylsiloxane (PDMS) material, polymer substrate, gasbag roller, and ultraviolet (UV) lamp. A DC (direct current) motor and lead screw control the velocity of the moving platform. The gasbag roller was fabricated by wrapping the sealed silicone tube around the aluminum roller. A gas inflated gasbag roller at particular gas pressure presses the belt type mold against the substrate.

Furthermore, external pressure was applied at both ends of the gasbag roller through a pneumatic cylinder. For the fabrication of belt-type mold of polydimethylsiloxane material, firstly, the polydimethylsiloxane solution was spin-coated on the embossed micro-lenses on polymer substrate followed by the baking process. Next, this polydimethylsiloxane film with micro-cavities was peeled off from the embossed micro-lenses. Finally, it is stuck on the belt-type PET (polyethylene terephthalate) film of 180 μm thickness with the help of silicon glue. After that, the UV (ultraviolet) lamp was turned on. Then, the gas bag roller was driven, and the UV (ultraviolet) resin-coated polymer substrate was moved via the moving platform to start the roller embossing. Finally, the gasbag roller was inflated at a gas pressure of 40 kPa, and 80 kPa of external pressure was applied at both sides of the gasbag roller shaft through a pneumatic cylinder.

The homogeneity in pressure distribution was examined using a pressure-sensitive film. This film was positioned at the location of the polymer substrate. The consequences of the internally and externally applied pressure on the precision of embossed micro-lenses were systematically investigated. This work shows that incomplete filling of mold was observed when inflated gas pressure was below 30 Kpa. This incomplete filling is due to the lower pressure, which was incapable of pressing the conveyor mold. Slip in embossed micro-patterns was observed when inner gas pressure is too high. This slip is due to higher gas pressure and lower contact area. The distortion in the embossed micro-lenses was observed when inner gas pressure was set at a high value. This distortion in embossed micro-lenses is due to a high value of internal

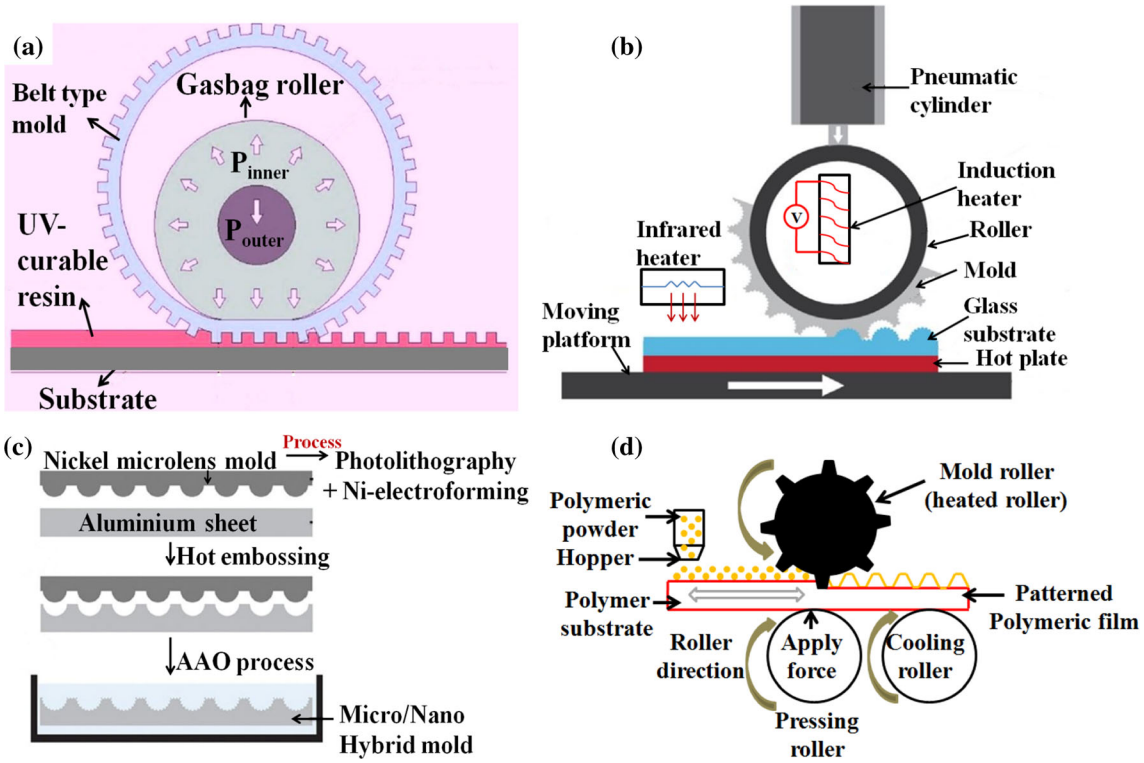

Fig. 20 **a** Schematic setup of UV-assisted gasbag roll to plate embossing, **b** Inductively coupled infrared assisted roll to plate hot embossing setup, **c** Detail fabrication procedure of micro-nano hierarchical pattern mold, and **d** Roll to roll hot powder embossing

gas pressure, which causes deformation in the micro-cavities on the PDMS (polydimethylsiloxane) mold. The profile of embossed micro-lenses was investigated using 2D and 3D surface profiler. The optical characteristic, i.e., FL (focal length), ROC (radius of curvature), and the numerical aperture of embossed micro-lenses, was measured by a light focusing system. This setup successfully fabricated micro-lenses of diameter = 95 μm, with a pitch = 200 μm and sag height = 9.5 μm. This setup is also helpful for manufacturing light guide plates at a cheap cost and high manufacturing rate (Wu and Yang 2010).

With the help of this setup, nano-scaled pillars were fabricated on a polycarbonate substrate. But in this case, seamless PDMS (polydimethylsiloxane) mold was used. These nano-scaled pores were developed in the internal part of an aluminum pipe through an anodic aluminum oxide process. Then PDMS solution was cast into it until its thickness reached 3 mm. This PDMS (polydimethylsiloxane) casted ring was cured at ambient temperature for 24 h, and a seamless PDMS (polydimethylsiloxane) mold was produced. Further, it was wrapped around the gas bag roller, and embossing was carried out. The anti-reflection effect and hydrophobicity effect of embossed polycarbonate film were investigated. After the embossing, the reflectance decreased from 14% (plain polycarbonate film) to 2% (nano-pattered polycarbonate film), and the contact angle or wetting angle increased from 77.5° (simple polycarbonate film) to 124.1° (nano-pattered polycarbonate film) (Lee et al. 2018).

4.7 Inductively coupled infrared (IR) assisted roll-to-plate hot embossing

Micro-lenses array is a primary part of optical devices (Kunnavakkam et al. 2003; Baroni et al. 2010), and its light transmission efficiency depends on the surface absorption and its reflection (Ko et al. 2011; Jung et al. 2011; Jung and Jeong 2012). Antireflection is achieved by fabricating nano-patterns on the surface of the micro-lenses array (Pacholski et al. 2012; Li et al. 2019b; Xie et al. 2019). For optical applications, glass is preferred over polymer due to its properties like high reflective index, negligible ultraviolet absorption, and high transmittance. In addition, it can work in higher temperatures and corrosive surroundings. Initially, the fabrications of micro/nano-patterns on glass substrate approaches like dry etching, maskless E-beam lithography, etc., were primarily used. But these processes are slow, time-consuming, complicated, considerably tedious, and can fabricate micro/nano-patterns in a limited area. Roller embossing solves these issues.

As already explained, Chih-Yuan Chang et al. (2006b) fabricated micro-lenses on a glass substrate by ultraviolet (UV)-assisted R2P-HE. In this case, the ultraviolet curable resin was spin-covered over the glass substrate, and then embossing was performed. This ultraviolet (UV) curable resin influences the fundamental optical properties of glass. Po-Lin Chen et al. (Chen et al. 2015) developed an inductively coupled infrared-assisted R2P-HE set up to fabricate the micro-lenses directly on a glass substrate. The setup is illustrated in Fig. 20b. With the help of this setup, anti-reflective micro-lenses were directly developed over a glass workpiece/substrate. This setup consists of a pneumatic cylinder, a steel roller integrated with an induction heater for heating the surface of the roller, and an infrared (IR) heater to pre-heat the upper surface of the glass. The lower surface of the glass was heated by the heated plate placed on the moving platform. The micro/nano-patterned cross mold was wrapped around the roller. The ceramic bearing was attached to the roller's two ends to prevent heat transfer from the roller to the pneumatic cylinder. The pneumatic cylinder applied pressure onto the roller through the ceramic bearing, and it presses the mold against the glass substrate. The temperature of the roller was observed continuously through infrared thermometers. The detailed fabrication procedure of the micro-nano hierarchical pattern mold is shown in Fig. 20c.

In the first fabrication stage, Nickel microlens mold was manufactured through lithography followed by the Ni-electroforming process. Next, embossing was carried out using Nickel microlens mold and aluminum sheet as a substrate. The micro-cavities were developed on the aluminum sheet, and this micro-patterned sheet was dipped into the electrolytic solution (phosphoric acid) for the anodic aluminum oxide (AAO) process. Thus nano-scaled pores were developed on the entire surface of the mold. The diameter of the pores varied as per changes in the anodizing voltage and the working temperature of the AAO (anodic aluminum oxide) process. This hybrid micro/nano-patterned steel mold was then wrapped around the cylinder. The hot plate and infrared heater preheated the glass substrate until the required temperature was reached. After attaining the required temperature, the embossing was started. The consequence of operational parameters on the quality of embossed anti-reflective micro-lenses was systematically investigated. The anti-reflection properties were investigated by measuring the spectral reflectance through the microscopic spectrometer. It is noted that the reflectance at the wavelength of 550 nm (sensitive to the human eye) reduced from 7.63 to 0.53%.

4.8 Roll-to-roll hot powder embossing (R2R-HPE)

In roll-to-roll hot powder embossing (R2R-HPE), the powder sintering process is combined with roll-to-roll hot embossing (R2R-HE). The powder sintering process has the advantage of near-final shape forming, and R2R-HE

promotes the continuous fabrication of micro-patterns on polymer substrate. The structures are made up of polymeric powder, while the base is the substrate that is fed. The schematic setup of the roll-to-roll hot powder embossing (R2R-HPE) is depicted in Fig. 20d.

The polymeric powder is fed through the hopper, and it moves along the polymer substrate. It passes through the micro-cavities (mold) on a roller with slight deformation during the embossing stage and is sintered before the deembossing stage. In this experiment, polyethylene powder of 29 µm particle size was used. The differential scanning calorimeter was used to measure melting temperature (133 °C) and specific heat (1.32 kJ/kg °C) of polyethylene powder. The nickel mold with micro-pyramid cavities was implemented, and a PET (polyethylene terephthalate) foil of 125 µm thick was used as a workpiece. During this process, many times, unmolten particles were leftover in the interior of the embossed micro-patterns. Therefore, unevenness was noticed in the embossed micro-pattern. To prevent this, a powder feeding model was designed according to the one-dimensional heat conduction equation. This model gives the relationship between the process parameters and maximum allowable powder quantity. Whenever feeding powder quantity is lower than the maximum permissible powder quantity, uniformity in the embossed micro-patterns was observed.

The process parameters like applied force (AF), embossing temperature (T_e), and feeding speed (FS) were modelled by response surface methodology; as the embossing temperature increases, the material flowability increases. When its temperature goes beyond the T_m, the polymer workpiece comes to the viscous flow state. Consequently, at greater values of T_e, the height of the embossed micro-patterns is close to the mold height. At the embossing load of 35 kgf, the porosity of the powder reaches zero, and the contact area increases due to the adequate compactness of the polymer powder. The ANOVA result confirms that T_e has more impact than the other two operating parameters. The optimum value of operating parameters was T_e of 135 °C, applied force (AF) of 3Kgf, and feeding speed (FS) of 0.4 m/min (Yi et al. 2018).

5 Commercial applications of hot embossing (HE)

The commercial applications of hot embossing are classified according to the domain where it is mainly used. It is primarily employed in the three domains, i.e., optical, biomedical, and micro-electro-mechanical systems (MEMS). The various commercial applications in this domain are listed in Table 1. Few applications of the hot embossing in the multiple domains are shown in Fig. 21.

6 Critical analysis of roller embossing

This segment sums up the previous discussion about the recent innovations in roller embossing and outlines the critical points of roller embossing techniques. The need for various roller embossing methods and their effectiveness in dealing with these limitations are better understood from this table. The critical analysis of roller embossing is encapsulated in Table 2.

7 Direction of future work

Research in roller-based hot embossing processes has begun relatively recently, around 2005 onwards. Therefore there is a lot of scopes in which the research can be progressed in this area. However, few of those approaches have been discussed here.

Sung-Won Youn et al. (2008) implemented an automatic mold releasing mechanism in roll-to-plate hot embossing. In contrast, HyungJun Lim et al. (2011) incorporated the movable press roller in roll-to-plate hot embossing. But in both setups, heating was carried out through the heating coil. For future research, the UV system may be implemented in these setups by merely coating the UV (ultraviolet) curable resin on polymer and implementing the UV source in the system. Consequently, embossing could be done at room temperature, and viscoelastic recovery in the embossed micro-pattern can be minimized.

Jarrett J. Dumond and Hong Yee Low (2012) developed a theoretical model for the time required for filling the micro-cavities during embossing. But this model is only applicable to uniform pressure distribution cases and infinitely long micro-cavities of width (w) and height (H). Future research on developing the theoretical model for the non-uniform pressure distribution and different micro-cavities shapes like circular, triangular, micro-pyramidal, etc., can be carried out. Ting et al. (2008b) developed the anti-reflection film by fabricating the conical, cylindrical array using the Ni-electroformed mold in the UV roller embossing. The average diameter, average height, and pitch of the conical-cylindrical array are equal to 200 nm, 350 nm, and 400 nm, respectively. In this case, the reflectance was achieved less than 2.45%. But currently, industries try to accomplish the reflectance of anti-reflection film below 0.1%. So in the future, there is scope to fabricate a nano-scaled conical-cylindrical array having all

Table 1 Commercial applications of hot embossing in various domains

Domain	Commercial applications of hot embossing	References
1.Optical	Micro-lens array	(Ong et al. 2002; Chang et al. 2006b, 2007)
	Anti-reflection film	(Ting et al. 2008a; Han et al. 2009; Yao et al. 2011; Jacobo-Martín et al. 2021)
	Light guided plate	(Yang and Huang 2012; Yang and Yang 2013; Wu et al. 2020; Wu and Liou 2021)
	Fresnel-lenses	(Hung et al. 2013; Weng and Huang 2013; Zhang et al. 2014b; Kuo and Chiang 2017)
	Brightness improvement film	(Wang and Tseng 2009; Yang and Huang 2013)
	Diffusive lighting panel	(Haponow et al. 2021)
	Optical waveguide	(Yoon 2004a, b; Bruck et al. 2013)
	Lenticular lens array for rising the viewing angle in the displays	(Ahn et al. 2007a)
	RGB colour filter for the LED display	(Liu and Chang 2007)
	Solar cell to enhance energy conversion efficiency	(Lee et al. 2021)
2. Biomedical	Micro-fluidic chip	(Ng et al. 2007; Nugen et al. 2009; Ng and Wang 2009; Chen et al. 2014; Asif et al. 2021),
	Deoxyribonucleic acid (DNA) separator	(Lee et al. 2001)
	DNA test	(Chen et al. 2005)
	Micro-containers for oral drug delivery	(Petersen et al. 2015; Abid et al. 2019)
	Micro-needles	(Abubaker and Zhang 2019; Li et al. 2019a)
	Biosensor	(Prada et al. 2019)
	Self-cleaning as well as an anti-biofouling surface achieved through fabricating the micro-patterns over the polymer surface	(Kung et al. 2009; Lee et al. 2013; Patil et al. 2019)
3. Micro electro-mechanical system	Micro-optical switches	(Shan et al. 2002, 2005; Murakoshi et al. 2003)
	Micro-nozzles	(Liao et al. 2017)
	Micro-reactors	(Metwally et al. 2012; Tollkötter et al. 2015)
	Enhance wear performance of coated tool	(Song et al. 2021)
	Electro-magnetic actuator	(Yun and Kim 2020)
	Micro-pumps	(Chee et al. 2012)

dimensions less than 10 nm (nm) and try to achieve the reflectance lower than 0.1%.

In thermal roller embossing, to increase the processing speed, it is essential to raise the roller mold temperature (T_{mold}) near the melting temperature ($T_{melting}$) of the polymer web to reduce the viscosity and filling time. But in this case, due to continuous embossing, it is tough to minimize the temperature of the embossed substrate below the T_g before the deembossing. Due to this, viscoelastic recovery took place, affecting the precision of the embossed micro-pattern. This viscoelastic recovery is acceptable in micron-scaled embossing, but it is not permitted in nano-scaled embossing. So there is future scope to implement an effective cooling system to achieve good accuracy in nano-scaled embossing through thermal roller embossing. In the future, this viscoelastic recovery can be reduced by minimizing the heating volume of the polymer substrate. It means only the polymer substrate, which comes in contact with roller mold, should be heated through the focused heating method.

In UV roller embossing, the anti-stick coating applied over the roller mold was degraded when exposed to a UV light source for a long time. To avoid this, soft roller molds manufactured from PDMS (polydimethylsiloxane) or ETFE (Ethylene tetrafluoroethylene) were used. In the future, there is scope to investigate the chemistry of anti-stick coating and UV curable resin so that the normal metallic mold with the anti-stick coating can be used in the UV roller embossing.

By taking motivation from modified setups of the traditional hot embossing (HE), the R2R-HE setup has already been modified. Researchers have systematically studied process parameters to evaluate the influence of operating parameters over replicability. The optimization of process parameters of an R2R-HE has been performed. Recently RSM (response surface methodology) has been applied to optimize R2R-HE parameters. In the future,

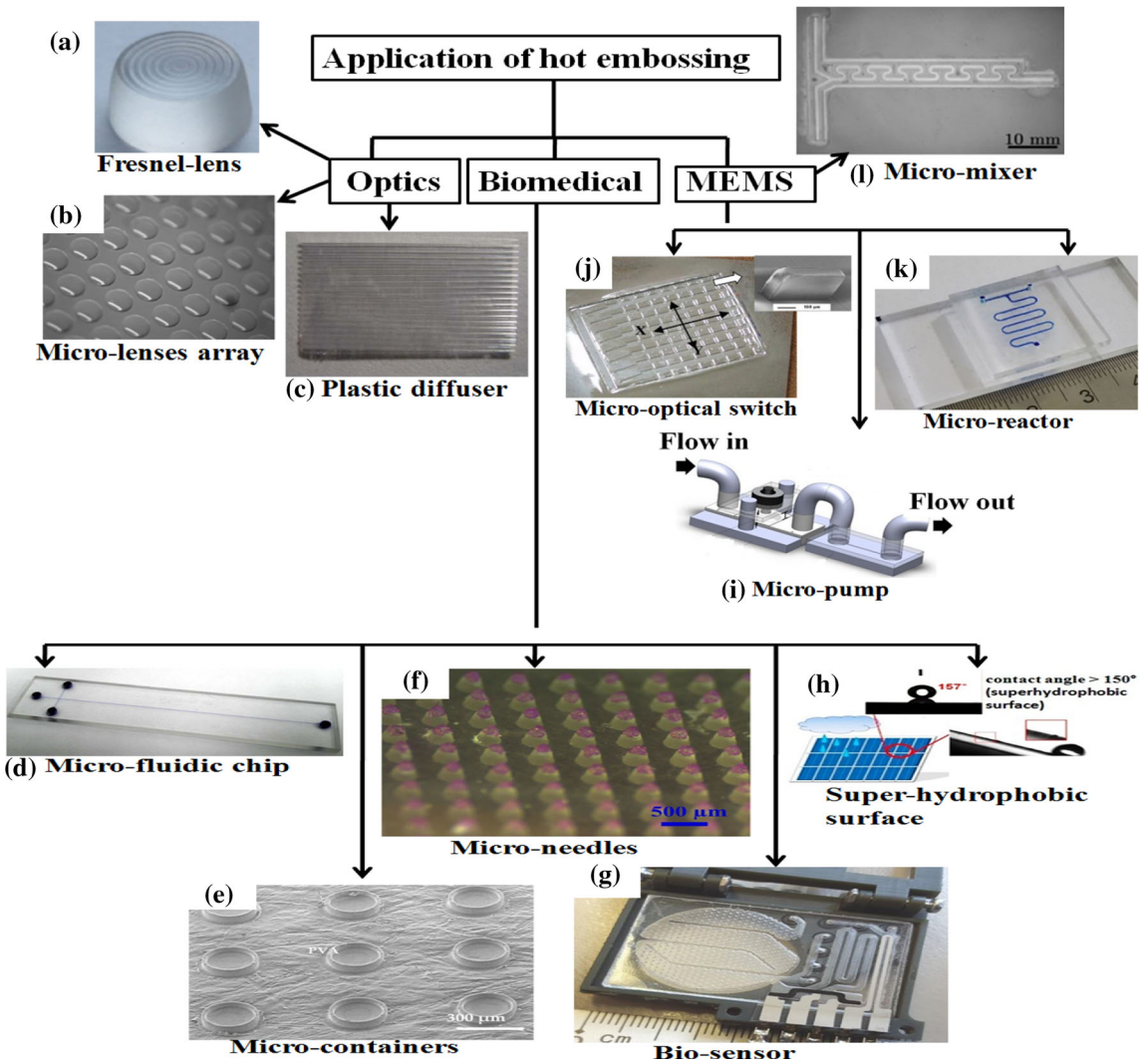

Fig. 21 Some applications of hot embossing in the various domains-**a** Fresnel lens (Hung et al. 2013), **b** micro-lenses array (Ong et al. 2002), **c** Plastic diffuser (Huang et al. 2008), **d** Micro-fluidic chip (Chen et al. 2014), **e** Micro-containers for oral drug delivery (Abid et al. 2019), **f** Micro-needle (Li et al. 2019a), **g** Bio-sensor (Prada et al. 2019), **h** Super-hydrophobic surface for self cleaning application (Lee et al. 2013), **i** Micro-pump (Chee et al. 2012), **j** Micro-optical switch (Shan et al. 2005), **k** micro-reactor (Sucularli et al. 2020), and **l** micro-mixer (Tollkötter et al. 2015)

advanced optimization techniques or nature-inspired optimization techniques may be used to attain better optimum results.

Fewer simulation-based studies have been carried out in roller embossing processes, and whatever work is available, it focuses on only one aspect of the process. There is a scope to work on this area.

8 Summary

This section summarizes the review article in graphical, numerical and statistical way. It is intended to help the researchers/scientist/readers to analyze data related to recent innovations in roller embossing. Figure 22a gives brief idea about the various micro-manufacturing processes used to fabricate the mold for embossing process. This graph shows the number of published articles in the respective year related to particular micro-manufacturing process. Figure 22b depicts percentile contribution of micro-manufacturing methods used to fabricate the mold for embossing process. From the analysis it is clear that majorly UV/X-ray/EBL followed by NE/RIE/WE have been used to fabricate the mold. But due to complexity of process researchers slowly moved towards non-conventional machining process i.e., micro-EDM, micro-milling etc. Figure 22c shows the number of articles published in the respective year related to the recent innovation in traditional hot embossing. From this it is clear that nowadays researchers are working on the induction aided hot

Table 2 Critical analysis of roller embossing

Sr. No.	Different roller embossing setups	Critical analysis
1	Roll to plate hot embossing with mold releasing mechanism and moving press roller	It is a batch-wise embossing process, but the area embossed in one cycle is still greater than conventional hot embossing. The embossing area in one cycle depends on the size of the mold
		An automatic mold releasing mechanism and moving press roller are incorporated to avoid distortion in the embossed micro-pattern
2	UV-assisted roll to plate hot embossing	In roll-to-plate hot embossing and its modified setup, a heating coil was used for heating purposes. It heats the polymer above T_g, and then it is rapidly cooled during deembossing. Because of this rapid cooling viscoelastic recovery takes place, which affects the replicability of the embossed structures
		To overcome this UV assisted roll-to-plate hot embossing was developed. UV-curable resin is spin-coated on the polymer substrate in this setup, and a UV source is used during the embossing. This process can be performed at room temperature, so there is no chance of viscoelastic recovery. This approach gives better replicability
		But this approach cannot be used to fabricate micro-patterns for biocompatible devices since UV curable resin is not chemically inert. Recently, to attain better pressure uniformity during the embossing stage, a gas-bag roller is implemented instead of a regular embossing roller to enhance the precision in the embossed micro-pattern
3	Roll to roll hot embossing	It is a continuous embossing process which is a big requirement of commercial manufacturing industries. But a roller-based manufacturing route has the issue of the presence of seam on the embossing roller, resulting in a discontinuity in the embossed micro-patterns
		Initially, trial and error are required to set the process parameters, especially roller speed and embossing temperature, at an optimum level. Different defects are present in the embossed substrate if the parameters are not set at the optimum level
4	Hybrid extrusion roll to roll hot embossing	It combines extrusion with the hot embossing process. In this case, extruded polymer at higher temperature is used as substrate and immediately passed through roll-to-roll hot embossing set up to carry out the embossing
		Because of this, the reheating of the substrate is not necessary, which lowers the developed thermal stresses in the embossed part and improves its thermal stability. Naturally, it is suitable for those industries which already have an extrusion setup
5	Double-sided roll to roll hot embossing	The embossing is carried out on both sides of the polymer substrate to achieve higher productivity. The simultaneous double-sided roll-to-roll hot embossing is preferred over the sequential double-sided roll-to-roll hot embossing since it gives better replicability
6	Infrared and inductive aided roll to roll hot embossing	Due to short allotted times for the embossing and deembossing stage, it is challenging to quickly heat and cool the embossing roller and polymer substrate in roll-to-roll hot embossing. As a result of that, viscoelastic recovery and distortion are observed in embossed micro-pattern
		To address this, only the surface of the embossing roller is heated in this approach, and the polymer substrate is preheated to a value that is just below the T_g before embossing. It gives better replicability in the embossed micro-patterns
7	Roll to roll hot powder embossing	The powder sintering process is merged with the roll-to-roll hot embossing process to attain near net shape and continuous embossing and minimize viscoelastic recovery in embossed micropattern
		The sintering process is carried out during the deembossing stage. To avoid the unmolten powder particles in the embossed micro-pattern, it is necessary to feed the powder quantity at optimum value. In this process, embossing temperature significantly affects embossed quality compared to the applied force and feeding speed of the polymer substrate

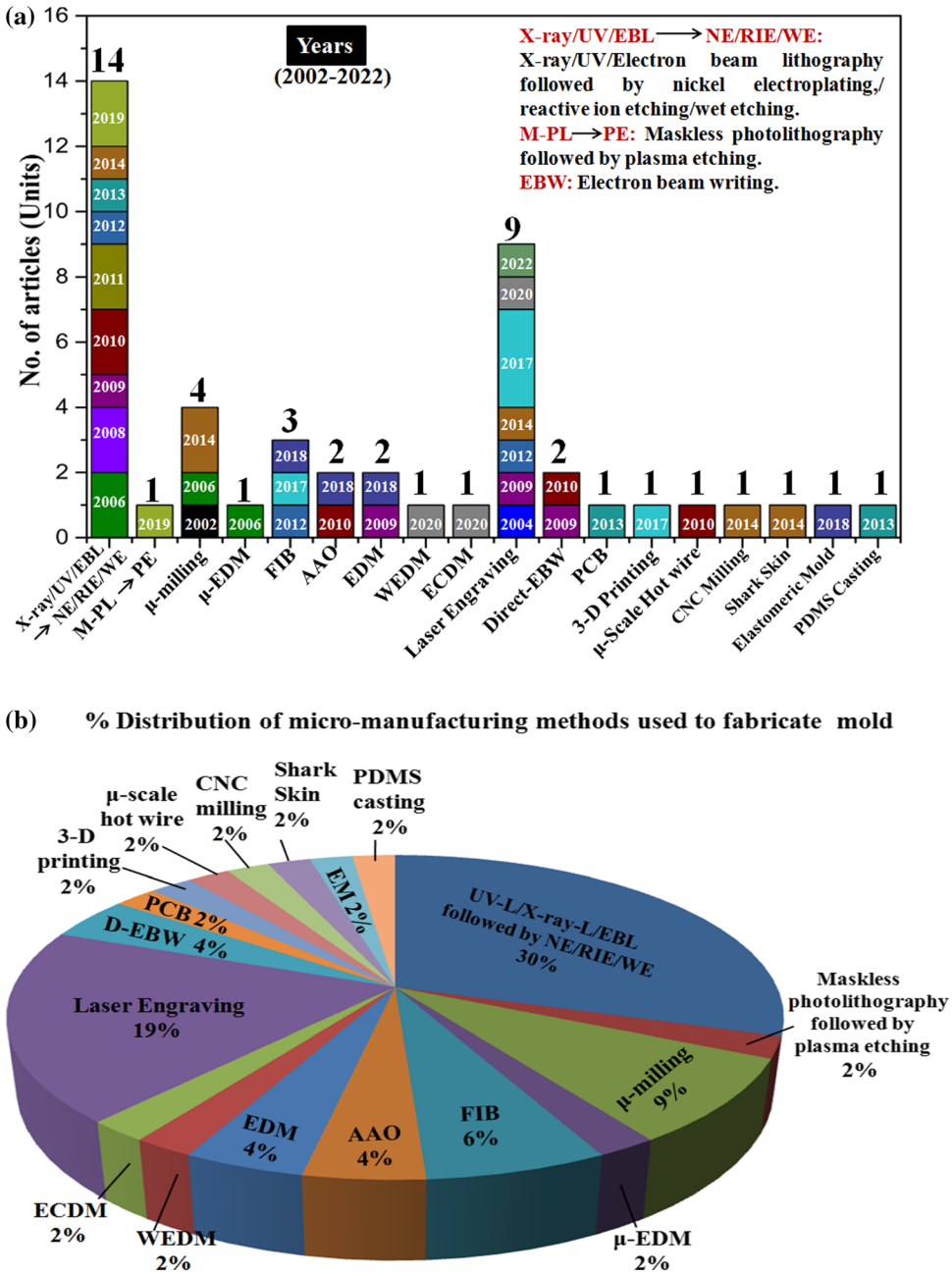

Fig. 22 **a** Number of articles published in the respective year related to various micro-manufacturing process used to fabricate the mold, **b** Percentile contribution of micro-manufacturing method used to fabricate the mold, **c** Number of articles published in the respective year related to the recent innovation in traditional hot embossing, **d** Percentile distribution of work related to recent innovation in traditional hot embossing, **e** Number of articles published in the respective year related to the recent innovation corresponding to the roller embossing, **f** Percentile contribution of work related to recent innovation in roller embossing

embossing and ultrasonic hot embossing as it setup minimizes embossing time from few minutes to few seconds and also enhances the replication by applying the embossing pressure uniformly. Figure 22d shows percentile distribution of work related to recent innovations in traditional hot embossing. Among all of these UHE contributes more i.e., 41%. Figure 21e depicts the graph related to the number of articles published in the respective year related to the recent innovation corresponding to the roller embossing. Most of the researchers worked on the thermal assisted R2R-HE followed by UV aided R2R-HE and Inductive aided R2R-HE. Recently researcher's focuses on induction aided R2R-HE setup. Figure 22f shows the percentile contribution of work related to recent innovation in roller embossing. The thermal assisted R2R-HE contributes more i.e., 36% of total innovations in RHE followed by UV aided R2R-HE (14%), and inductive aided R2R-HE (10%).

Fig. 22 continued

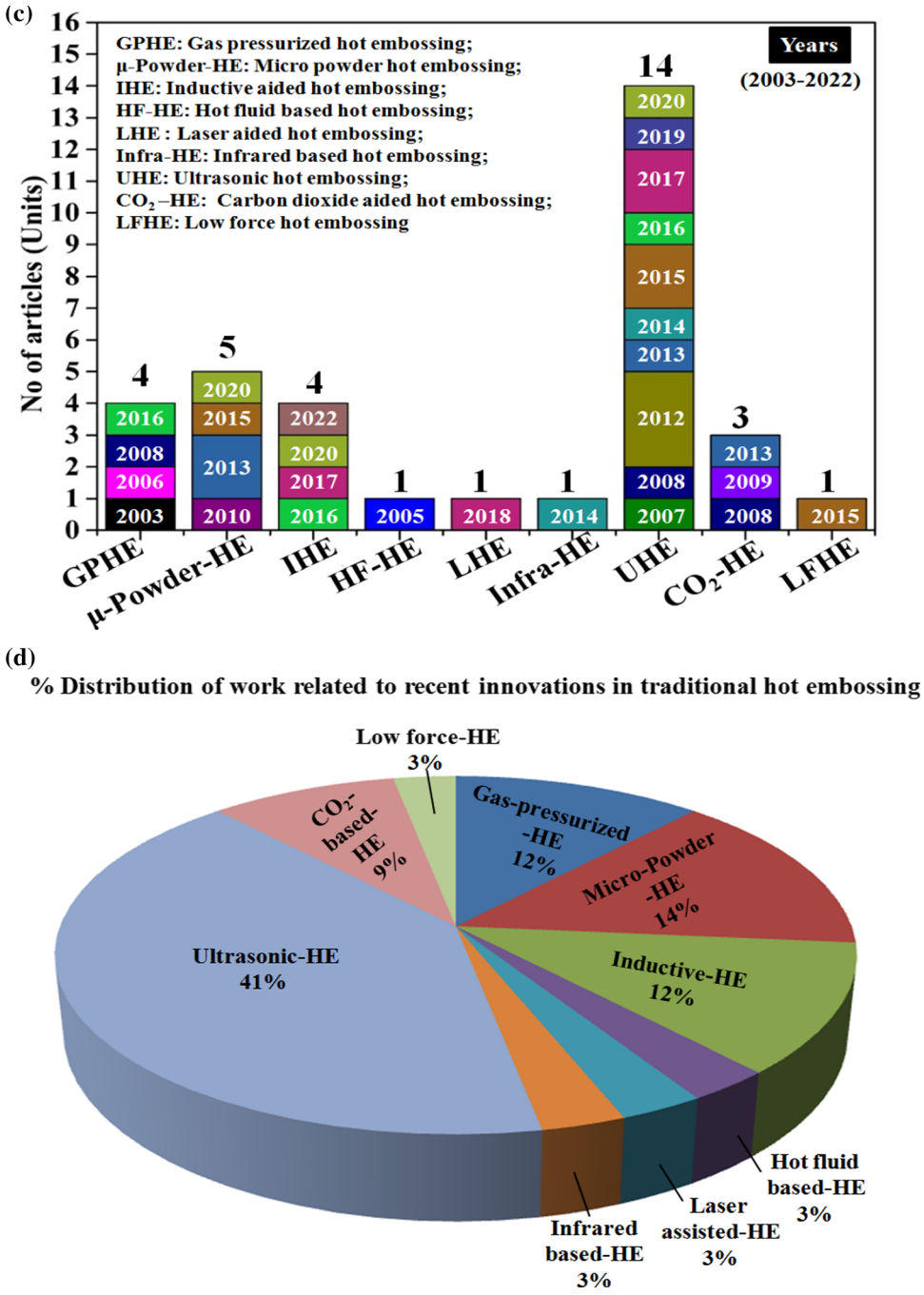

9 Conclusions

To fabricate micron and nano scaled patterns over a large area of the polymer web, industries focus on developing a manufacturing process capable of manufacturing these patterns on a large scale. Roller embossing is one of the processes having cheap cost as well as a high output. It overcomes the issue of batch mode embossing that arises in the traditional hot embossing. Roller embossing, especially UV roller embossing, can achieve nano-scaled patterns with high precision over a large area. It is complicated to fabricate with traditional hot embossing (HE) because of the viscoelastic recovery of polymer in traditional hot embossing. The important conclusions of this comprehensive review are summarized as follow:

(1) Continuous embossing of the thermoplastic polymer with thermally assisted roller embossing is a favourable method because of the tool setup and versatility of the polymer material. Ample heat, optimum pressure, an appropriate roller mold, and

Fig. 22 continued

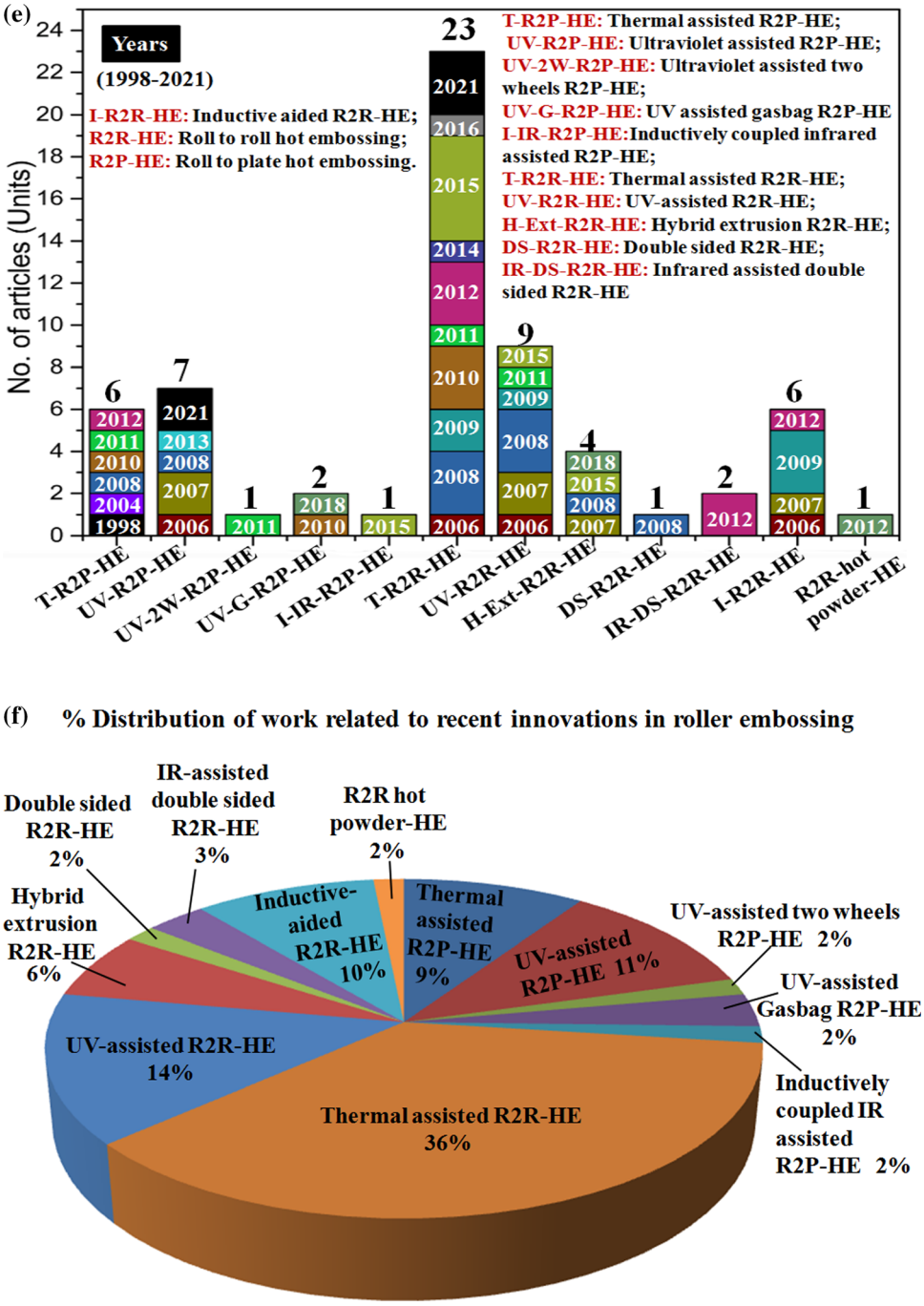

thermoplastic polymer that can be embossed directly are required for proper replication of micropatterns over the surface of the polymer. In thermally-assisted roller embossing, the polymer web embossed directly, eliminating the need to place a medium over the polymer surface like UV roller embossing and eliminating the additional processing stages, like a uniform deposition, spreading of resin over the substrate. The methodology is often versatile in the selection of materials. The roller mold is manufactured through different materials, and various varieties of polymer substrate may be used. Additionally, semi-conductive polymers and luminous polymers that are embossed directly with this method are not easy to achieve with UV roller embossing. The chemistry needed for curing process affects its functionality.

(2) The thermally-assisted roller embossing with seamless roller mold, useful for the broad area embossing with less time, ultimately reduces the manufacturing

cost of commercial applications like an array of micro-lenses, displays, anti-reflection films, hydrophobic surface, etc.

(3) The UV roller embossing requires less pressure to replicate the micro-patterns over the mold onto the workpiece than thermally-assisted roller embossing. Because of the low pressure, the accumulating type of defects arising from the residues or dust particles in the mold is avoided. Thus, it helps to enhance the mold life and improves replication quality. In addition, due to the low pressure, soft mold fabricated from polydimethylsiloxane (PDMS) and ethylene tetrafluoroethylene (ETFE) materials having low surface energy can be used. Because of this, it is not necessary to apply an anti-stick coating over the mold.

(4) In UV roller embossing, UV curable resin was used; this UV curable resin does not have T_g like polymer material used in thermal roller embossing. Therefore UV curable resin does not undergo viscoelastic recovery at a particular temperature. Thus, with the help of UV roller embossing, it can fabricate the nano-scaled patterns with precision over the polymer web.

(5) It is necessary to implement the roller mold, polymer web, and backing roller free from surface waviness and non-uniformities in the UV roller embossing. Otherwise, the non-uniformities are easily transferred over the UV curable resin during the process and result in an uneven residual layer and underfilling of the cavity over the mold.

(6) To replicate a complex profile over a large area, roll-to-plate hot embossing was developed. This setup is further modified by implementing an automatic mold releasing mechanism and movable press roller to enhance the replicability by minimizing distortion in the deembossing stage. To minimize viscoelastic recovery observed after deembossing, ultraviolet (UV) curable R2P-HE was developed in which embossing could be performed at T_o (room temperature). But still, R2P-HE is a noncontinuous and batch-wise manufacturing process. In addition, the size of the mold limits the area embossed per cycle.

(7) For continuous embossing of micro-patterns on a polymer web/workpiece, R2R-HE was developed. The roller speed, T_e, and P_e were found to affect the replication quality significantly. In addition, due to the absence of the cooling process in the deembossing stage, thermal reflow was observed. It reduces the accuracy of the embossed part obtained after embossing.

(8) Different types of defects like bubble, platform, and collapse type defects were observed in R2R-HE. The root cause of this defect is the improper setting of process parameters. The shape-preserving mechanism was studied to minimize such defects, and a systematic study of process parameters was carried out. The experimentation shows that a higher value of a tensile force of shape-preserving unit results in higher wrap angle and contact pressure. Therefore, it leads to a longer flow time helps to improve replicability. The working temperature range extended from 135 to 170 °C and feeding speed (FS) of polymer from 0.5 to 2.5 m/min through the shape-preserving mechanism. Recently optimization of process parameters of R2R-HE has been performed to find the optimal level of working parameters and the impact of individual working parameters on the replicability.

Acknowledgements This work was supported by the Science and Engineering Research Board (SERB) (a statutory body of the Department of Science and Technology, Government of India) under Grant [SRG/2019/002093(vide diary no. SERB/F/6926/2019-2020)].

References

Abid Z, Dalskov Mosgaard M, Manfroni G et al (2019) Investigation of mucoadhesion and degradation of PCL and PLGA microcontainers for oral drug delivery. Polymers (basel) 11:1828. https://doi.org/10.3390/polym11111828

Abubaker SS, Zhang Y (2019) Optimization design and fabrication of polymer micro needle by hot embossing method. Int J Precis Eng Manuf 20:631–640. https://doi.org/10.1007/s12541-019-00095-z

Ahn SH, Guo LJ (2008) High-Speed Roll-to-Roll Nanoimprint Lithography on Flexible Plastic Substrates. Adv Mater 20:2044–2049. https://doi.org/10.1002/adma.200702650

Ahn SH, Guo LJ (2009) Large-area roll-to-roll and roll-to-plate Nanoimprint Lithography: a step toward high-throughput application of continuous nanoimprinting. ACS Nano 3:2304–2310. https://doi.org/10.1021/nn9003633

Ahn S, Cha J, Myung H et al (2006) Continuous ultraviolet roll nanoimprinting process for replicating large-scale nano- and micropatterns. Appl Phys Lett 89:18–21. https://doi.org/10.1063/1.2392960

Ahn S, Choi M, Bae H et al (2007a) Design and fabrication of micro optical film by ultraviolet roll imprinting. Japanese J Appl Physics, Part 1 Regul Pap Short Notes Rev Pap 46:5478–5484. https://doi.org/10.1143/JJAP.46.5478

Ahn SH, Kim J-S, Guo LJ (2007b) Bilayer metal wire-grid polarizer fabricated by roll-to-roll nanoimprint lithography on flexible plastic substrate. J Vac Sci Technol B Microelectron Nanom Struct 25:2388. https://doi.org/10.1116/1.2798747

Ali MY, Mohammad AS (2009) Effect of conventional EDM parameters on the micromachined surface roughness and fabrication of a hot embossing master microtool. Mater Manuf Process 24:454–458. https://doi.org/10.1080/10426910802714373

Asif M, Tait RN, Berini P (2021) Hot embossing of microfluidics in cyclic-olefin co-polymer using a wafer aligner-bonder. Microsyst Technol. https://doi.org/10.1007/s00542-020-05188-8

Baroni PY, Paivanranta B, Scharf T et al (2010) Nanostructured surface fabricated by laser interference lithography to attenuate the reflectivity of microlens arrays. J Eur Opt Soc Rapid Publ 5:10006. https://doi.org/10.2971/jeos.2010.10006

Becker H, Dietz W (1998) Microfluidic devices for μ -TAS applications fabricated by polymer hot embossing. In: Frazier AB, Ahn CH (eds) Microfluidic devices and systems, Proc. SPIE 3515, pp 177–182. https://doi.org/10.1117/12.322081

Becker H, Heim U (2000) Hot embossing as a method for the fabrication of polymer high aspect ratio structures. Sensors Actuators, A Phys 83:130–135. https://doi.org/10.1016/S0924-4247(00)00296-X

Bhavsar SN, Aravindan S, Rao PV (2012) Machinability study of cemented carbide using focused ion beam (FIB) milling. Mater Manuf Process 27:1029–1034. https://doi.org/10.1080/10426914.2011.654166

Bruck R, Muellner P, Kataeva N et al (2013) Flexible thin-film polymer waveguides fabricated in an industrial roll-to-roll process. Appl Opt 52:4510. https://doi.org/10.1364/AO.52.004510

Chan-Park MB, Neo WK (2003) Ultraviolet embossing for patterning high aspect ratio polymeric microstructures. Microsyst Technol 9:501–506. https://doi.org/10.1007/s00542-002-0289-0

Chang CY, Hu BW (2018) Experimental study of hybrid extrusion rolling embossing process for replicating large-area micropattern devices. Int J Adv Manuf Technol 95:1003–1012. https://doi.org/10.1007/s00170-017-1293-y

Chang C-Y, Tsai M-H (2015) Development of a continuous roll-to-roll processing system for mass production of plastic optical film. J Micromech Microeng 25:125014. https://doi.org/10.1088/0960-1317/25/12/125014

Chang JH, Yang SY (2003) Gas pressurized hot embossing for transcription of micro-features. Microsyst Technol 10:76–80. https://doi.org/10.1007/s00542-003-0311-1

Chang JH, Yang SY (2005) Development of fluid-based heating and pressing systems for micro hot embossing. Microsyst Technol 11:396–403. https://doi.org/10.1007/s00542-004-0481-5

Chang CY, Yang SY, Chu MH (2007) Rapid fabrication of ultraviolet-cured polymer microlens arrays by soft roller stamping process. Microelectron Eng 84:355–361. https://doi.org/10.1016/j.mee.2006.11.004

Chang CY, Yang SY, Huang LS, Chang JH (2006a) Fabrication of plastic microlens array using gas-assisted micro-hot-embossing with a silicon mold. Infrared Phys Technol 48:163–173. https://doi.org/10.1016/j.infrared.2005.10.002

Chang CY, Yang SY, Sheh JL (2006b) A roller embossing process for rapid fabrication of microlens arrays on glass substrates. Microsyst Technol 12:754–759. https://doi.org/10.1007/s00542-006-0103-5

Chee PS, Arsat R, Adam T et al (2012) Modular architecture of a non-contact pinch actuation micropump. Sensors (switzerland) 12:12572–12587. https://doi.org/10.3390/s120912572

Chee PS, Arsat R, Hashim U et al (2013) Micropump pattern replication using Printed Circuit Board (PCB) technology. Mater Manuf Process 28:702–706. https://doi.org/10.1080/10426914.2012.736664

Chen PL, Hong RH, Yang SY (2015) Hot-rolled embossing of microlens arrays with antireflective nanostructures on optical glass. J Micromech Microeng 25:95001. https://doi.org/10.1088/0960-1317/25/9/095001

Chen Q, Zhang L, Chen G (2014) Far infrared-assisted embossing and bonding of poly(methyl methacrylate) microfluidic chips. RSC Adv 4:56440–56444. https://doi.org/10.1039/c4ra09909e

Chen SC, Lin MC, Chien RD, Liaw WL (2005) Hot embossing of micro-featured devices. In: Proc 2005 IEEE Int Conf Mechatronics, ICM '05 2005:777–782. https://doi.org/10.1109/ICMECH.2005.1529360

Cheng G, Sahli M, Gelin JC, Barriere T (2014) Process parameter effects on dimensional accuracy of a hot embossing process for polymer-based micro-fluidic device manufacturing. Int J Adv Manuf Technol 75:225–235. https://doi.org/10.1007/s00170-014-6135-6

Chien RD (2006) Hot embossing of microfluidic platform. Int Commun Heat Mass Transf 33:645–653. https://doi.org/10.1016/j.icheatmasstransfer.2006.01.017

Chuang CH, Lu DM, Wang PH et al (2018) Antireflective polymer films via roll to roll UV nanoimprint lithography using an AAO mold. Microsyst Technol 24:389–395. https://doi.org/10.1007/s00542-017-3299-7

Deng Y, Yi P, Peng L et al (2014) Experimental investigation on the large-area fabrication of micro-pyramid arrays by roll-to-roll hot embossing on PVC film. J Micromech Microeng 24:045023. https://doi.org/10.1088/0960-1317/24/4/045023

Deng Y, Yi P, Peng L et al (2015) Flow behavior of polymers during the roll-to-roll hot embossing process. J Micromech Microeng 25:65004. https://doi.org/10.1088/0960-1317/25/6/065004

Deshmukh SS, Goswami A (2020a) Investigation of deviation in width of embossed micro-structure by hot embossing. IOP Conf Ser Mater Sci Eng 872:12069. https://doi.org/10.1088/1757-899x/872/1/012069

Deshmukh SS, Goswami A (2020b) Hot embossing of polymers—a review. Mater Today Proc 26:405–414. https://doi.org/10.1016/j.matpr.2019.12.067

Deshmukh SS, Goswami A (2021) Recent developments in hot embossing—a review. Mater Manuf Process 36:501–543. https://doi.org/10.1080/10426914.2020.1832691

Deshmukh SS, Goswami A (2022) Microlens array through induction-aided hot embossing: fabrication, optimization, and characterization. Mater Manuf Process 00:1–15. https://doi.org/10.1080/10426914.2022.2030876

Du G, Yang Q, Chen F et al (2012) Direct fabrication of seamless roller molds with gapless and shaped-controlled concave microlens arrays. Opt Lett 37:4404. https://doi.org/10.1364/ol.37.004404

Dumond JJ, Yee Low H (2012) Recent developments and design challenges in continuous roller micro- and nanoimprinting. J Vac Sci Technol b, Nanotechnol Microelectron Mater Process Meas Phenom 30:010801. https://doi.org/10.1116/1.3661355

Emadinia O, Vieira MT, Vieira MF (2020) Micro powder hot embossing of aluminum feedstock. J Mater Eng Perform. https://doi.org/10.1007/s11665-020-04869-9

Eom H, Park K (2009) Fully-coupled numerical analysis of high-frequency induction heating for thin-wall injection molding. Polym Plast Technol Eng 48:1070–1077. https://doi.org/10.1080/03602550903092484

Fagan MD, Kim BH, Yao D (2009) A novel process for continuous thermal embossing of large-area nanopatterns onto polymer films. Adv Polym Technol 28:246–256. https://doi.org/10.1002/adv.20167

Forfang WBD, Conner TG, You BH et al (2014) Fabrication and characterization of polymer microprisms. Microsyst Technol 20:2071–2077. https://doi.org/10.1007/s00542-014-2067-1

Gan Z, Yu Z, Chen Z, Chen G (2010) Hot embossing of electrophoresis microchannels in PMMA substrates using electric heating wires. Anal Bioanal Chem 396:2715–2720. https://doi.org/10.1007/s00216-010-3490-5

Gerlach A, Knebel G, Guber AE et al (2002) Microfabrication of single-use plastic microfluidic devices for high-throughput screening and DNA analysis. Microsyst Technol 7:265–268. https://doi.org/10.1007/s005420100114

Gomez JA, Conner GT, Chun DH et al (2014) Mold filling analysis of an alignment structure in micro hot embossing. Fibers Polym 15:1197–1201. https://doi.org/10.1007/s12221-014-1197-5

Goswami A, Singh K, Aravindan S, Rao PV (2017) Optimizing FIB milling process parameters for silicon and its use in nanoreplication. Mater Manuf Process 32:1052–1058. https://doi.org/10.1080/10426914.2016.1257127

Goswami A, Umashankar R, Gupta AK et al (2018) Development of a microstructured surface using the FIB. J Micromanufacturing 1:53–61. https://doi.org/10.1177/2516598418765357

Guo C, Feng L, Zhai J et al (2004) Large-area fabrication of a nanostructure-induced hydrophobic surface from a hydrophillic polymer. ChemPhysChem 5:750–753. https://doi.org/10.1002/cphc.200400013

Habermehl A, Brenner P, Huber R et al (2019) Roll-to-roll hot embossing of 1D and 2D photonic nanostructures. Adv Eng Mater 21:1–8. https://doi.org/10.1002/adem.201900110

Han KS, Lee H, Kim D, Lee H (2009) Fabrication of anti-reflection structure on protective layer of solar cells by hot-embossing method. Sol Energy Mater Sol Cells 93:1214–1217. https://doi.org/10.1016/j.solmat.2009.01.002

Haponow L, Kettle J, Allsop J (2021) Optimization of a continuous hot embossing process for fabrication of micropyramid structures in thermoplastic sheets. J Vac Sci Technol B 39:012203. https://doi.org/10.1116/6.0000551

He Y, Wu W, Zhang T, Fu J (2015) Micro structure fabrication with a simplified hot embossing method. RSC Adv 5:39138–39144. https://doi.org/10.1039/c5ra01410g

Heckele M, Bacher W, Hanemann T, Ulrich H (1997) Hot embossing and injection molding for microoptical components. In: Frank WF (ed) Proc. SPIE 3135, Precision plastic optics for optical storage, displays, imaging, and communications. pp 24–29

Heckele M, Bacher W, Müller KD (1998) Hot embossing—The molding technique for plastic microstructures. Microsyst Technol 4:122–124. https://doi.org/10.1007/s005420050112

Hocheng H, Wen TT, Yang SY (2008) Replication of microlens arrays by gas-assisted hot embossing. Mater Manuf Process 23:261–268. https://doi.org/10.1080/10426910701860830

Hong-Wei C, Yung-Chun L, Fei-Bin H (2010) Fabrication of seamless patterns onto metal rollers by photolithography. In: 2010 IEEE 5th International Conference on Nano/Micro Engineered and Molecular Systems. IEEE, pp 887–892

Hu C-N, Hsieh H-T, Su G-DJ (2011) Fabrication of microlens arrays by a rolling process with soft polydimethylsiloxane molds. J Micromech Microeng 21:065013. https://doi.org/10.1088/0960-1317/21/6/065013

Huang K-F, Lee Y-C (2013) Fabrication of metal roller mold with submicrometer feature size using contact printing photolithography technique. J Vac Sci Technol B 31:031604. https://doi.org/10.1116/1.4804275

Huang M-S, Tai N-S (2009) Experimental rapid surface heating by induction for micro-injection molding of light-guided plates. J Appl Polym Sci 113:1345–1354

Huang T-C, Chan B-D, Ciou J-K, Yang S-Y (2009) Fabrication of microlens arrays using a CO 2 -assisted embossing technique. J Micromech Microeng 19:015018. https://doi.org/10.1088/0960-1317/19/1/015018

Huang T-C, Ciou J-R, Huang P-H et al (2008) Fast fabrication of integrated surface-relief and particle-diffusing plastic diffuser by use of a hybrid extrusion roller embossing process. Opt Express 16:440. https://doi.org/10.1364/oe.16.000440

Hung JC, Tsai YP, Hung C (2013) Development of a new apparatus for ultrasonic vibration-assisted glass hot embossing process. Precis Eng 37:222–227. https://doi.org/10.1016/j.precisioneng.2012.06.002

Hupert ML, Guy WJ, Llopis SD et al (2006) Evaluation of micromilled metal mold masters for the replication of microchip electrophoresis devices. Microfluid Nanofluidics 3:1–11. https://doi.org/10.1007/s10404-006-0091-x

Idei K, Ishizawa N, Noda D, Hattori T (2006) Development of roll metal mold by synchrotron radiation. In: 2006 IEEE International Symposium on MicroNanoMechanical and Human Science. IEEE, pp 1–6

Ishizawa N, Idei K, Kimura T et al (2008) Resin micromachining by roller hot embossing. Microsyst Technol 14:1381–1388. https://doi.org/10.1007/s00542-007-0552-5

Jacobo-Martín A, Rueda M, Hernández JJ et al (2021) Bioinspired antireflective flexible films with optimized mechanical resistance fabricated by roll to roll thermal nanoimprint. Sci Rep 11:1–15. https://doi.org/10.1038/s41598-021-81560-6

Jaszewski RW, Schift H, Gobrecht J, Smith P (1998) Hot embossing in polymers as a direct way to pattern resist. Microelectron Eng 41–42:575–578. https://doi.org/10.1016/S0167-9317(98)00135-X

Jiang L-T, Huang T-C, Chiu C-R et al (2007) Fabrication of plastic microlens arrays using hybrid extrusion rolling embossing with a metallic cylinder mold fabricated using dry film resist. Opt Express 15:12088. https://doi.org/10.1364/OE.15.012088

Jung H, Jeong K-H (2012) Monolithic polymer microlens arrays with antireflective nanostructures. Appl Phys Lett 101:203102. https://doi.org/10.1063/1.4747717

Juang Y-J, Lee LJ, Koelling KW (2002a) Hot embossing in microfabrication. Part i: Experimental Polym Eng Sci 42:539–550. https://doi.org/10.1002/pen.10970

Juang Y-J, Lee LJ, Koelling KW (2002b) Hot embossing in microfabrication. Part II: rheological characterization and process analysis. Polym Eng Sci 42:551–566. https://doi.org/10.1002/pen.10971

Jung H, Song C, Jeong K-H (2011) Monolithic polymer microlens arrays with anti-reflective structures using a metal annealed mask. In: 16th International Conference on Optical MEMS and Nanophotonics. IEEE, pp 145–146

Jung W, Lee H-J, Park K (2015) Investigation of localized heating characteristics in selective ultrasonic imprinting. Int J Precis Eng Manuf 16:1999–2004. https://doi.org/10.1007/s12541-015-0260-5

Jung W, Ra J, Park K (2012) Design optimization of ultrasonic horn for micro-pattern replication. Int J Precis Eng Manuf 13:2195–2201. https://doi.org/10.1007/s12541-012-0291-0

Kao C-C, Ke K-C, Hung W-C, Yang S-Y (2020) Hot embossing of microstructure with moving induction heating and gas-assisted pressuring. Microsyst Technol 26:957–967. https://doi.org/10.1007/s00542-019-04560-7

Kim BI, Lee KG, Lee TJ et al (2013a) A continuous tilting of micromolds for fabricating polymeric microstructures in microinjection. Lab Chip 13:4321–4325. https://doi.org/10.1039/C3LC50494H

Kim M, Moon B-U, Hidrovo CH (2013b) Enhancement of the thermo-mechanical properties of PDMS molds for the hot embossing of PMMA microfluidic devices. J Micromech Microeng 23:095024. https://doi.org/10.1088/0960-1317/23/9/095024

Kim S, Shiau C-S, Kim BH, Yao D (2007) Injection molding nanoscale features with the aid of induction heating. Polym Plast Technol Eng 46:1031–1037. https://doi.org/10.1080/03602550701522344

Kim S, Son Y, Park H et al (2015) Effects of preheating and cooling durations on roll-to-roll hot embossing. Microsc Microanal 21:164–171. https://doi.org/10.1017/S1431927614013324

Kimerling TE, Liu W, Kim BH, Yao D (2006) Rapid hot embossing of polymer microfeatures. Microsyst Technol 12:730–735. https://doi.org/10.1007/s00542-006-0098-y

Kimerling TE, Yao D, Kim BH (2009) Injection molding poly(paraphenylene) with a rapidly heated mold. Polym Plast Technol Eng 48:1008–1013. https://doi.org/10.1080/03602550903092518

Ko D-H, Tumbleston JR, Henderson KJ et al (2011) Biomimetic microlens array with antireflective "moth-eye" surface. Soft Matter 7:6404. https://doi.org/10.1039/c1sm05302g

Kodihalli Shivaprakash N, Ferraguto T, Panwar A et al (2019a) Fabrication of flexible polymer molds for polymer microstructuring by roll-to-roll hot embossing. ACS Omega 4:12480–12488. https://doi.org/10.1021/acsomega.9b01468

Kodihalli Shivaprakash N, Zhang J, Nahum T et al (2019b) Roll-to-roll hot embossing of high aspect ratio micro pillars for superhydrophobic applications. Int Polym Process 34:502–512. https://doi.org/10.3139/217.3815

Kolew A, Münch D, Sikora K, Worgull M (2011) Hot embossing of micro and sub-micro structured inserts for polymer replication. Microsyst Technol 17:609–618. https://doi.org/10.1007/s00542-010-1182-x

Kosloh J, Sackmann J, Šakalys R et al (2017a) Heat generation and distribution in the ultrasonic hot embossing process. Microsyst Technol 23:1411–1421. https://doi.org/10.1007/s00542-016-2836-0

Kosloh J, Sackmann J, Schomburg WK (2017b) Ultrasonic fabrication of micro fluidic channels from polyether ether ketone (PEEK). Microsyst Technol 23:5505–5513. https://doi.org/10.1007/s00542-017-3284-1

Kumar N, Mandal N, Das AK (2020) Micro-machining through electrochemical discharge processes: a review. Mater Manuf Process 35:363–404. https://doi.org/10.1080/10426914.2020.1711922

Kung KY, Horng JT, Chiang KT (2009) Material removal rate and electrode wear ratio study on the powder mixed electrical discharge machining of cobalt-bonded tungsten carbide. Int J Adv Manuf Technol 40:95–104. https://doi.org/10.1007/s00170-007-1307-2

Kunnavakkam MV, Houlihan FM, Schlax M et al (2003) Low-cost, low-loss microlens arrays fabricated by soft-lithography replication process. Appl Phys Lett 82:1152–1154. https://doi.org/10.1063/1.1555694

Kuo CC, Chiang TS (2017) Development of a precision hot embossing tool with microstructures for microfabrication. Int J Adv Manuf Technol 91:1321–1326. https://doi.org/10.1007/s00170-016-9859-7

Kurita T, Ogura I, Ashida K (2018) Proposal of laser assisted hot embossing technology for glass. J Mater Process Technol 254:248–253. https://doi.org/10.1016/j.jmatprotec.2017.11.040

Lan S, Song JH, Lee MG et al (2010) Continuous roll-to-flat thermal imprinting process for large-area micro-pattern replication on polymer substrate. Microelectron Eng 87:2596–2601. https://doi.org/10.1016/j.mee.2010.07.021

Lang V, Rank A, Lasagni AF (2017) Direct laser interference patterning of metallic sleeves for roll-to-roll hot embossing. In: Klotzbach U, Washio K, Kling R (eds) Laser-based micro- and nanoprocessing XI, Proc. SPIE 10092, p 100920T. https://doi.org/10.1117/12.2252623

Lee GB, Chen SH, Huang GR et al (2001) Microfabricated plastic chips by hot embossing methods and their applications for DNA separation and detection. Sensors Actuators, B Chem 75:142–148. https://doi.org/10.1016/S0925-4005(00)00745-0

Lee D, Tang YL, Liu SJ (2021) Fast fabrication of nanostructured films using nanocolloid lithography and UV soft mold roller embossing: effects of processing parameters. Polymers (basel) 13:1–14. https://doi.org/10.3390/polym13030405

Lee H-J, Park K (2016) Variable wettability control of a polymer surface by selective ultrasonic imprinting and hydrophobic coating. Colloid Polym Sci 294:1413–1423. https://doi.org/10.1007/s00396-016-3902-y

Lee HJ, Park K (2014) Development of composite micro-patterns on polymer film using repetitive ultrasonic imprinting. Int J Precis Eng Manuf - Green Technol 1:341–345. https://doi.org/10.1007/s40684-014-0043-y

Lee S-H, Han K-S, Shin J-H et al (2013) Fabrication of highly transparent self-cleaning protection films for photovoltaic systems. Prog Photovoltaics Res Appl 21:1056–1062. https://doi.org/10.1002/pip.2203

Lee Y-C, Chen H-W, Hsiao F-B (2012) Fabrication of seamless roller mold for continuous roller imprinting of microlens array films. J Microelectromech Syst 21:316–323. https://doi.org/10.1109/JMEMS.2011.2178115

Lee YC, Chen PC, Lin HY (2009) Fabrication of seamless roller mold with excimer laser direct writing technology. In: 4th IEEE Int Conf Nano/Micro Eng Mol Syst NEMS 2009 767–770. https://doi.org/10.1109/NEMS.2009.5068691

Lee YH, Ke KC, Chang NW, Yang SY (2018) Development of an UV rolling system for fabrication of micro/nano structure on polymeric films using a gas-roller-sustained seamless PDMS mold. Microsyst Technol 24:2941–2948. https://doi.org/10.1007/s00542-017-3683-3

Li J, Chen D, Chen G (2005) Low-temperature thermal bonding of PMMA microfluidic chips. Anal Lett 38:1127–1136. https://doi.org/10.1081/AL-200057209

Li J, Zhou Y, Yang J et al (2019a) Fabrication of gradient porous microneedle array by modified hot embossing for transdermal drug delivery. Mater Sci Eng C 96:576–582. https://doi.org/10.1016/j.msec.2018.11.074

Li Y, Park S, Fullager DB et al (2019b) Near-infrared transmittance enhancement using fully conformal antireflective structured surfaces on microlenses fabricated by direct laser writing. Opt Eng 58:010501. https://doi.org/10.1117/1.OE.58.1.010501

Li K, Xu G, Huang X et al (2018) Manufacturing of Micro-lens array using contactless micro-embossing with an EDM-Mold. Appl Sci 9:85. https://doi.org/10.3390/app9010085

Li K, Xu G, Luo H et al (2020) Glass flow behaviors in microchannels during hot embossing. Ceram Int. https://doi.org/10.1016/j.ceramint.2020.05.253

Li W-H, Chen H-W, Hu Y-W, et al (2011) Fabrication of seamless roller molds using step-and-rotate curved surface photolithography and application on micro-lens array optic film. In: 2011 6th IEEE International Conference on Nano/Micro Engineered and Molecular Systems. IEEE, pp 728–731

Liao S, Gerhardy C, Sackmann J, Schomburg WK (2015) Tools for ultrasonic hot embossing. Microsyst Technol 21:1533–1541. https://doi.org/10.1007/s00542-014-2232-6

Liao S, Sackmann J, Tollkötter A et al (2017) Ultrasonic fabrication of micro nozzles from a stack of PVDF foils for generating and characterizing microfluidic dispersions. Microsyst Technol 23:695–702. https://doi.org/10.1007/s00542-015-2708-z

Lim H, Choi KB, Kim G et al (2011) Roller nanoimprint lithography for flexible electronic devices of a sub-micron scale. Microelectron Eng 88:2017–2020. https://doi.org/10.1016/j.mee.2011.02.018

Lin TY, Do T, Kwon P, Lillehoj PB (2017) 3D printed metal molds for hot embossing plastic microfluidic devices. Lab Chip 17:241–247. https://doi.org/10.1039/c6lc01430e

Liu S-J, Huang C-C, Liao C-T (2012) Continuous infrared-assisted double-sided roll-to-roll embossing of flexible polymer substrates. Polym Eng Sci 52:1395–1401. https://doi.org/10.1002/pen.23068

Liu S-J, Liaw C-T (2012) Fast fabrication of nano-structured anti-reflection layers for enhancement of solar cells performance using plasma sputtering and infrared assisted roller embossing

techniques. Opt Express 20:5143. https://doi.org/10.1364/oe.20.005143
Liu SJ, Chang YC (2007) A novel soft-mold roller embossing method for the rapid fabrication of micro-blocks onto glass substrates. J Micromech Microeng 17:172–179. https://doi.org/10.1088/0960-1317/17/1/022
Mäkelä T, Haatainen T, Majander P et al (2008) Continuous double-sided roll-to-roll imprinting of polymer film. Jpn J Appl Phys 47:5142–5144. https://doi.org/10.1143/JJAP.47.5142
Mappes T, Worgull M, Heckele M, Mohr J (2008) Submicron polymer structures with X-ray lithography and hot embossing. Microsyst Technol 14:1721–1725. https://doi.org/10.1007/s00542-007-0499-6
Mekaru H, Nakamura O, Maruyama O et al (2007) Development of precision transfer technology of atmospheric hot embossing by ultrasonic vibration. Microsyst Technol 13:385–391. https://doi.org/10.1007/s00542-006-0203-2
Mekaru H, Noguchi T, Goto H, Takahashi M (2008) Effect of applying ultrasonic vibration in thermal nanoimprint lithography. Microsyst Technol 14:1325–1333. https://doi.org/10.1007/s00542-007-0512-0
Mekaru H, Yamada T, Yan S, Hattori T (2004) Microfabrication by hot embossing and injection molding at LASTI. Microsyst Technol 10:682–688. https://doi.org/10.1007/s00542-004-0401-8
Metwally K, Robert L, Queste S et al (2012) Roll manufacturing of flexible microfluidic devices in thin PMMA and COC foils by embossing and lamination. Microsyst Technol 18:199–207. https://doi.org/10.1007/s00542-011-1358-z
Murakoshi Y, Shan XC, Maeda R (2003) Application of micro hot embossing for mems structures. Int J Comput Eng Sci 04:617–620. https://doi.org/10.1142/s1465876303001897
Nagato K, Sugimoto S, Hamaguchi T, Nakao M (2010) Iterative roller imprint of multilayered nanostructures. Microelectron Eng 87:1543–1545. https://doi.org/10.1016/j.mee.2009.11.029
Nezuka O, Yao D, Kim BH (2008) Replication of microstructures by roll-to-roll UV-curing embossing. Polym Plast Technol Eng 47:865–873. https://doi.org/10.1080/03602550802189001
Ng SH, Wang ZF (2008) Hot roller embossing for the creation of microfluidic devices. In: 2008 Symposium on Design, Test, Integration and Packaging of MEMS/MOEMS. IEEE, pp 262–266
Ng SH, Wang ZF (2009) Hot roller embossing for microfluidics: process and challenges. Microsyst Technol 15:1149–1156. https://doi.org/10.1007/s00542-008-0722-0
Ng SH, Wang ZF, Tjeung RT, De Rooij NF (2007) Development of a multi-layer microelectrofluidic platform. Microsyst Technol 13:1509–1515. https://doi.org/10.1007/s00542-006-0341-6
Nian SC, Tsai TH, Huang MS (2016) Novel inductive hot embossing for increasing micromolding efficiency. Int Commun Heat Mass Transf 70:38–46. https://doi.org/10.1016/j.icheatmasstransfer.2015.11.005
Niino H, Ding X, Kurosaki R et al (2004) Imprinting by hot embossing in polymer substrates using a template of silica glass surface-structured by the ablation of LIBWE method. Appl Phys A 79:827–828. https://doi.org/10.1007/s00339-004-2820-x
Nugen SR, Asiello PJ, Baeumner AJ (2009) Design and fabrication of a microfluidic device for near-single cell mRNA isolation using a copper hot embossing master. Microsyst Technol 15:477–483. https://doi.org/10.1007/s00542-008-0694-0
Ong NS, Koh YH, Fu YQ (2002) Microlens array produced using hot embossing process. Microelectron Eng 60:365–379. https://doi.org/10.1016/S0167-9317(01)00695-5
Pacholski C, Morhard C, Spatz JP et al (2012) Antireflective subwavelength structures on microlens arrays—comparison of various manufacturing techniques. Appl Opt 51:8. https://doi.org/10.1364/AO.51.000008
Pan CT, Su CH (2008a) Fabrication of high fill factor optical film using two-layer photoresists. J Mod Opt 55:33–42. https://doi.org/10.1080/09500340701260032
Pan CT, Su CY (2008b) Study of micro-lens array by reflow process. J Mod Opt 55:2843–2856. https://doi.org/10.1080/09500340802226536
Park YM, Shin HG, Gang M et al (2011) Fabrication of hemispherical nanopatterns on 3D microsurface. Mater Res Innov 15:s347–s351. https://doi.org/10.1179/143307511X12858957674715
Park YW, Kim TW (2014) Evaluation of microforming methods for shark skin replication. Mater Res Innov. https://doi.org/10.1179/1432891714Z.000000000518
Patil D, Sharma A, Aravindan S, Rao PV (2019) Development of hot embossing setup and fabrication of ordered nanostructures on large area of polymer surface for antibiofouling application. Micro Nano Lett 14:191–195. https://doi.org/10.1049/mnl.2018.5462
Peng L, Wu H, Shu Y et al (2016) Roll-to-roll hot embossing system with shape preserving mechanism for the large-area fabrication of microstructures. Rev Sci Instrum 87:105120. https://doi.org/10.1063/1.4963907
Petersen RS, Mahshid R, Andersen NK et al (2015) Hot embossing and mechanical punching of biodegradable microcontainers for oral drug delivery. Microelectron Eng 133:104–109. https://doi.org/10.1016/j.mee.2014.11.009
Piotter V, Mueller K, Plewa K et al (2002) Performance and simulation of thermoplastic micro injection molding. Microsyst Technol 8:387–390. https://doi.org/10.1007/s00542-002-0178-6
Prada J, Cordes C, Harms C, Lang W (2019) Design and manufacturing of a disposable, cyclo-olefin copolymer, microfluidic device for a biosensor †. Sensors 19:1178. https://doi.org/10.3390/s19051178
Qi N, Luo Y, Wang XD et al (2015) Local thermal-assisted ultrasonic embossing for the fabrication of polymer microstructures. Microsyst Technol 21:1101–1110. https://doi.org/10.1007/s00542-014-2306-5
Qi N, Luo Y, Yan X et al (2013) Using silicon molds for ultrasonic embossing on Polymethyl Methacrylate (PMMA) substrates. Microsyst Technol 19:609–616. https://doi.org/10.1007/s00542-012-1671-1
Rank A, Lang V, Lasagni AF (2017) High-speed roll-to-roll hot embossing of micrometer and sub micrometer structures using seamless direct laser interference patterning treated sleeves. Adv Eng Mater 19:1–8. https://doi.org/10.1002/adem.201700201
Sahli M, Gelin JC (2013) Development of a feedstock formulation based on polypropylene for micro-powder soft embossing process of 316L stainless steel micro-channel part. Int J Adv Manuf Technol 69:2139–2148. https://doi.org/10.1007/s00170-013-5170-z
Sahli M, Gelin JC, Barrière T (2010) Numerical modelling of the Polymers replication in micro-cavities by the roll embossing process. Int J Mater Form 3:607–610. https://doi.org/10.1007/s12289-010-0843-8
Sahli M, Khan Malek C, Geli JC (2009) 3D modelling and simulation of the filling of cavities by viscoelastic polymer in roll embossing process. Int J Mater Form 2:725–728. https://doi.org/10.1007/s12289-009-0542-5
Scheer HC, Schulz H (2001) A contribution to the flow behaviour of thin polymer films during hot embossing lithography. Microelectron Eng 56:311–332. https://doi.org/10.1016/S0167-9317(01)00569-X
Schelb M, Vannahme C, Kolew A, Mappes T (2011) Hot embossing of photonic crystal polymer structures with a high aspect ratio.

J Micromech Microeng 21:025017. https://doi.org/10.1088/0960-1317/21/2/025017
Schift H, David C, Gabriel M et al (2000) Nanoreplication in polymers using hot embossing and injection molding. Microelectron Eng 53:171–174. https://doi.org/10.1016/S0167-9317(00)00289-6
Schift H, Halbeisen M, Schütz U et al (2006) Surface structuring of textile fibers using roll embossing. Microelectron Eng 83:855–858. https://doi.org/10.1016/j.mee.2006.01.120
Seo YS, Park K (2012) Direct patterning of micro-features on a polymer substrate using ultrasonic vibration. Microsyst Technol 18:2053–2061. https://doi.org/10.1007/s00542-012-1524-y
Shan X, Soh YC, Shi CWP et al (2009) A micro roller embossing process for structuring large-area substrates of laminated ceramic green tapes. Microsyst Technol 15:1319–1325. https://doi.org/10.1007/s00542-008-0739-4
Shan X, Soh YC, Shi CWP et al (2008) Large-area patterning of multilayered green ceramic substrates using micro roller embossing. J Micromech Microeng 18:065007. https://doi.org/10.1088/0960-1317/18/6/065007
Shan XC, Ikehara T, Murakoshi Y, Maeda R (2005) Applications of micro hot embossing for optical switch formation. Sensors Actuators, A Phys 119:433–440. https://doi.org/10.1016/j.sna.2004.09.026
Shan XC, Maeda R, Murakoshi Y (2002) Development of a micro hot embossing process for fabricating micro-optical devices. Nano-Microtechnol Mater Process Packag Syst 4936:67. https://doi.org/10.1117/12.469430
Shen YK, Chang HJ, Hung LH (2007) Analysis of the replication properties of lightguiding plate for micro injection compression molding. Key Eng Mater 329:643–648. https://doi.org/10.4028/www.scientific.net/KEM.329.643
Shih YM, Kao CC, Ke KC, Yang SY (2017) Imprinting of double-sided microstructures with rapid induction heating and gas-assisted pressuring. J Micromech Microeng. https://doi.org/10.1088/1361-6439/aa7acd
Soh YC, Shan X, Lu CW (2008) Process Challenges for Realization of High Quality Roller Embossing for Patterning Large Area Green Ceramic Substrates. In: 2008 10th Electronics Packaging Technology Conference. IEEE, pp 109–114
Song X, Jian Y, Zou W et al (2021) Preparation and characterization of coated abrasives with domed pyramid thermosetting polyurethane/epoxy/diamond composites by roller embossing: Wear performance. Diam Relat Mater 120:108632. https://doi.org/10.1016/j.diamond.2021.108632
Song X, Shan XC, Chow SL et al (2015) Numerical and experimental study of the filling stage of roll-to-roll UV embossing process with micro features. Microsyst Technol 21:1729–1738. https://doi.org/10.1007/s00542-014-2290-9
Su Y-C, Shah J, Lin L (2003) Implementation and analysis of polymeric microstructure replication by micro injection molding. J Micromech Microeng 14:415–422. https://doi.org/10.1088/0960-1317/14/3/015
Sucularli F, Arikan MAS, Yildirim E (2020) Investigation of process-affected zone in ultrasonic embossing of microchannels on thermoplastic substrates. J Manuf Process 50:394–402. https://doi.org/10.1016/j.jmapro.2019.12.055
Tan H (1998) Roller nanoimprint lithography. J Vac Sci Technol B Microelectron Nanom Struct 16:3926. https://doi.org/10.1116/1.590438
Taniguchi J, Aratani M (2009) Fabrication of a seamless roll mold by direct writing with an electron beam on a rotating cylindrical substrate. J Vac Sci Technol B Microelectron Nanom Struct 27:2841. https://doi.org/10.1116/1.3237141
Taniguchi J, Tsuji S, Aratani M (2010) Fabrication of seamless three-dimensional roll mold using direct electron-beam writing on rotating cylindrical substrate. J Vac Sci Technol B 28:C6M45-C6M49. https://doi.org/10.1116/1.3511474
Ting C-J, Huang M-C, Tsai H-Y et al (2008a) Low cost fabrication of the large-area anti-reflection films from polymer by nanoimprint/hot-embossing technology. Nanotechnology 19:205301. https://doi.org/10.1088/0957-4484/19/20/205301
Ting CJ, Chang FY, Chen CF, Chou CP (2008b) Fabrication of an antireflective polymer optical film with subwavelength structures using a roll-to-roll micro-replication process. J Micromech Microeng. https://doi.org/10.1088/0960-1317/18/7/075001
Tollkötter A, Sackmann J, Baldhoff T et al (2015) Ultrasonic hot embossed polymer microreactors for optical measurement of chemical reactions. Chem Eng Technol 38:1113–1121. https://doi.org/10.1002/ceat.201400522
Tsai YP, Hung JC, Yin LC, Hung C (2012) Ultrasonic vibration-assisted optical glass hot embossing process. Int J Adv Manuf Technol 60:1207–1213. https://doi.org/10.1007/s00170-011-3669-8
Tsao CW, Chen TY, Woon WY, Lo CJ (2012) Rapid polymer microchannel fabrication by hot roller embossing process. Microsyst Technol 18:713–722. https://doi.org/10.1007/s00542-012-1513-1
Velten T, Bauerfeld F, Schuck H et al (2011) Roll-to-roll hot embossing of microstructures. Microsyst Technol 17:619–627. https://doi.org/10.1007/s00542-010-1158-x
Wan L, Zhu N, Li X et al (2016) Optimization for solid polymer microstructure replication using gas-assisted hot embossing under low pressure. Int J Precis Eng Manuf 17:1067–1072. https://doi.org/10.1007/s12541-016-0129-2
Wang J, Yi P, Deng Y et al (2015) Mechanism of forming defects in roll-to-roll hot embossing of micro-pyramid arrays: II. Numerical Study. J Micromech Microeng 25:115030. https://doi.org/10.1088/0960-1317/25/11/115030
Wang M-W, Tseng C-C (2009) Analysis and fabrication of a prism film with roll-to-roll fabrication process. Opt Express 17:4718. https://doi.org/10.1364/OE.17.004718
Weng YC, Weng YJ, Yang SY (2011) Electromagnetic field-aided magnetic soft mold reverse imprinting technology applied in microstructure replication. Polym - Plast Technol Eng 50:1077–1083. https://doi.org/10.1080/03602559.2010.531425
Weng YJ, Huang JC (2013) A discussion on the development of SCF-CO2 hot embossing molding technology and replication moldability. Polym - Plast Technol Eng 52:539–545. https://doi.org/10.1080/03602559.2012.762376
Wong YC, Weng YJ, Weng YC, Lee JY (2010) Development and study of applications combining nanopowder imprint lithography and array-type UV-curing technology for micro-lens molding. Polym - Plast Technol Eng 49:853–860. https://doi.org/10.1080/03602551003664602
Worgull M, Heckele M, Schomburg WK (2005) Large-scale hot embossing. Microsyst Technol 12:110–115. https://doi.org/10.1007/s00542-005-0012-z
Worgull M, Hétu JF, Kabanemi KK, Heckele M (2006) Modeling and optimization of the hot embossing process for micro- and nanocomponent fabrication. Microsyst Technol 12:947–952. https://doi.org/10.1007/s00542-006-0124-0
Wu CH, Kuo HC (2007) Parametric study of injection molding and hot embossing in polymer microfabrication. J Mech Sci Technol 21:1477–1482. https://doi.org/10.1007/BF03177362
Wu CH, Liou YC (2021) The use of roll-to-plate UV-curing embossing to produce a composite light guide plate. Microsyst Technol. https://doi.org/10.1007/s00542-020-05184-y
Wu J-T, Yang S-Y (2010) A gasbag-roller-assisted UV imprinting technique for fabrication of a microlens array on a PMMA substrate. J Micromech Microeng 20:085038. https://doi.org/10.1088/0960-1317/20/8/085038

Wu J-T, Chang W-Y, Yang S-Y (2010a) Fabrication of a nano/micro hybrid lens using gas-assisted hot embossing with an anodic aluminum oxide (AAO) template. J Micromech Microeng 20:075023. https://doi.org/10.1088/0960-1317/20/7/075023

Wu JT, Chu YT, Yang SY, Li CC (2010b) Low-temperature embossing technique for fabrication of large-area polymeric microlens array with supercritical carbon dioxide. Microelectron Eng 87:2620–2624. https://doi.org/10.1016/j.mee.2010.07.028

Wu CH, Chiu CH, Chen YH (2020) Design and application of a hybrid alignment platform for a double-sided hot embossing process. Microsyst Technol 26:721–730. https://doi.org/10.1007/s00542-019-04563-4

Xie S, Wan X, Yang B et al (2019) Design and fabrication of wafer-level microlens array with moth-eye antireflective nanostructures. Nanomaterials 9:747. https://doi.org/10.3390/nano9050747

Yang C-H, Yang S-Y (2013) A high-brightness light guide plate with high precise double-sided microstructures fabricated using the fixed boundary hot embossing technique. J Micromech Microeng 23:035033. https://doi.org/10.1088/0960-1317/23/3/035033

Yang J-C, Huang C-C (2012) Using UV roll-to-plate imprint lithography to fabricate light guide plates with microdot patterns. Micro Nano Lett 7:244. https://doi.org/10.1049/mnl.2012.0097

Yang JC, Huang CC (2013) Fabrication of dual brightness enhancement structures on light guide plates using UV roll-to-plate imprinting lithography. Optik (stuttg) 124:3324–3328. https://doi.org/10.1016/j.ijleo.2012.10.049

Yang H-P, Shen Y-K, Lin Y (2014) Replication of plastic thin film by microfeature mould in large area hot embossing. Plast Rubber Compos 43:39–45. https://doi.org/10.1179/1743289813Y.0000000068

Yang S-Y, Huang T-C, Ciou J-K et al (2008) CO 2 -assisted embossing for the fabrication of PMMA components under low temperature and with low pressure. J Micromech Microeng 18:025024. https://doi.org/10.1088/0960-1317/18/2/025024

Yao D, Kimerling TE, Kim B (2006) High-frequency proximity heating for injection molding applications. Polym Eng Sci 46:938–945. https://doi.org/10.1002/pen.20548

Yao TF, Wu PH, Wu TM et al (2011) Fabrication of anti-reflective structures using hot embossing with a stainless steel template irradiated by femtosecond laser. Microelectron Eng 88:2908–2912. https://doi.org/10.1016/j.mee.2011.03.023

Yeo LP, Ng SH, Wang Z et al (2009) Micro-fabrication of polymeric devices using hot roller embossing. Microelectron Eng 86:933–936. https://doi.org/10.1016/j.mee.2008.12.021

Yeo LP, Ng SH, Wang ZF et al (2010) Investigation of hot roller embossing for microfluidic devices. J Micromech Microeng 20:015017. https://doi.org/10.1088/0960-1317/20/1/015017

Yi P, Deng Y, Shu Y, Peng L (2018) Experimental studies on a novel roll-to-roll powder hot embossing for large-area fabrication of micropyramid arrays on polymers. J Micromech Microeng 28:085007. https://doi.org/10.1088/1361-6439/aabe10

Yi P, Shu Y, Deng Y et al (2015) Mechanism of forming defects in roll-to-roll hot embossing of micro-pyramid arrays I: Experiments. J Micromech Microeng 25:105017. https://doi.org/10.1088/0960-1317/25/10/105017

Yoon KB (2004a) Fabrication of multimode polymeric waveguides by hot embossing process: effect of sidewall roughness on insertion loss. Macromol Res 12:437–442. https://doi.org/10.1007/BF03218424

Yoon KB (2004b) Low-loss polymeric waveguides having large cores fabricated by hot embossing and micro-contact printing techniques. Macromol Res 12:474–477. https://doi.org/10.1007/BF03218429

Youn SW, Ogiwara M, Goto H et al (2008) Prototype development of a roller imprint system and its application to large area polymer replication for a microstructured optical device. J Mater Process Technol 202:76–85. https://doi.org/10.1016/j.jmatprotec.2007.08.069

Yun D, Kim M (2020) Development of an electromagnetic actuator for the hot-embossing process. Electronics 9:948. https://doi.org/10.3390/electronics9060948

Yun D, Son Y, Kyung J et al (2012) Development of roll-to-roll hot embossing system with induction heater for micro fabrication. Rev Sci Instrum 83:015108. https://doi.org/10.1063/1.3675574

Zhang J, Gelin J-C, Sahli M, Barrière T (2013) Manufacturing of 316L stainless steel die mold by hot embossing process for microfluidic applications. J Micro Nano-Manufacturing 1:1–10. https://doi.org/10.1115/1.4025554

Zhang J, Sahli M, Gelin JC, Barriere T (2015) Rapid replication of metal microstructures using micro-powder hot embossing process. Int J Adv Manuf Technol 77:2135–2149. https://doi.org/10.1007/s00170-014-6595-8

Zhang J, Sahli M, Gelin JC, Khan-Malek C (2014a) Rapid-manufacturing of micro-structured devices based on MWCNTs/PP composites by using hot embossing replication process. Microsyst Technol 20:1919–1924. https://doi.org/10.1007/s00542-013-1999-1

Zhang X, Liu K, Shan X, Liu Y (2014b) Roll-to-roll embossing of optical linear Fresnel lens polymer film for solar concentration. Opt Express 22:A1835. https://doi.org/10.1364/oe.22.0a1835

Zhong ZW, Ng HH, Chen SH, Shan XC (2018) Hot roller embossing of multi-dimensional microstructures using elastomeric molds. Microsyst Technol 24:1443–1452. https://doi.org/10.1007/s00542-017-3584-5

Zhong ZW, Shan XC (2012) Microstructure formation via roll-to-roll UV embossing using a flexible mould made from a laminated polymer–copper film. J Micromech Microeng 22:085010. https://doi.org/10.1088/0960-1317/22/8/085010

Zhong ZW, Shan XC, Lim YZ (2015) The edge-effect on roll-to-roll thermal embossing of micro channels. Microsyst Technol 21:1267–1273. https://doi.org/10.1007/s00542-014-2245-1

Zhong ZW, Shan XC, Wong SJ (2011) Roll-to-roll large-format slot die coating of photosensitive resin for UV embossing. Microsyst Technol 17:1703–1711. https://doi.org/10.1007/s00542-011-1344-5

Zhu J, Tian Y, Yang C et al (2017) Low-cost and fast fabrication of the ultrasonic embossing on polyethylene terephthalate (PET) films using laser processed molds. Microsyst Technol 23:5653–5668. https://doi.org/10.1007/s00542-017-3369-x

Zou W, Sackmann J, Striegel A et al (2019) Comparison of hot embossing micro structures with and without ultrasound. Microsyst Technol 25:4185–4195. https://doi.org/10.1007/s00542-019-04469-1